Investigating Triplet Transfer in Singlet Fission – Low Bandgap Semiconductor Bilayers using Magnetic Field Effects

Bachelor Thesis

by

Fabian Ecker

submitted at

Universität Konstanz

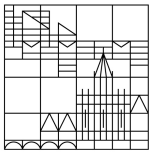

conducted at

AMOLF physics of functional complex matter

Faculty of Science

Department of Physics

Hybrid Solar Cells group

Examiner:
Prof. Dr. Lukas Schmidt-Mende

Supervisor:
Dr. Bruno Ehrler

Daily Supervisor:
Benjamin Daiber

Amsterdam, September 2019

Zusammenfassung

Mit Hinblick auf die globale Erwärmung gewinnen regenerative Energiequellen wie Sonne und Wind immer mehr an Bedeutung. Besonders die Nutzung von Solarenergie durch Photovoltaik wird auf dem zukünftigen Energiemarkt eine große Rolle spielen.
In organischen Halbleitern, die den sogenannten *Singlet Fission* Prozess durchlaufen, führt die Absorption eines hochenergetischen Photons zur Anregung von zwei Elektronen-Loch-Paaren (Exzitonen). Dies ist ein vielversprechendes Phänomen, das in der Photovoltaikforschung genutzt werden kann, um eine Effizienzsteigerung von Solarzellen zu erreichen.
In dieser Arbeit werden die Magnetfeldeffekte von Singlet Fission Materialien untersucht. Die Intensität der Photolumineszenz von Singlet Fission Materialien ändert sich auf eine spezielle Art, wenn ein äußeres Magnetfeld angelegt wird. Die Beobachtung dieses Effekts ist eine gute Methode, um neue Materialien ausfindig zu machen, die den Singlet Fission Prozess durchlaufen.
Mit dieser Methodik wurden Perylendiimide (PDI) mit unterschiedlichen funktionalen Gruppen ausfindig gemacht, die Singlet Fission betreiben. Die Anordnung der PDI-Moleküle spielt dabei eine Rolle, inwiefern sich die Singlet Fission Effizienz bei unterschiedlichen Magnetfeldstärken verhält.
Mit der Zusammenführung von Singlet Fission Materialien und herkömmlichen Solarzellenmaterialien kann erreicht werden, dass Exzitonen vom organischen in den anorganischen Halbleiter übergehen, was eine Effizienzsteigerung der Solarzellen zur Folge hat.
Es wurde untersucht, ob Exzitonen vom Singlet Fission Material Tetracen in ein Solarzellenmaterial übergehen, wenn eine Doppelschicht aus beiden Materialien vorliegt. Dabei wurde herausgefunden, dass die Intensität der Photolumineszenz des Solarzellenmaterials mit der Anzahl an Exzitonen im Tetracen gekoppelt ist. Dies kann entweder mit einem Exzitonenübergang oder einem Photonenübergang zwischen den Materialien erklärt werden.

Abstract

Because of the increasing demand of renewable energy sources regarding global warming, photovoltaics are gaining more importance than ever in recent years. *Singlet fission* is an energy down conversion process occurring in certain organic semiconductors. By the generation of two excitons after the absorption of one photon it is an effect promising to enhance the efficiency of solar cells.
In this thesis the magnetic field effects of singlet fission materials are investigated by observing the photoluminescence of samples. The photoluminescence intensity of singlet fission material changes in a certain way when an external magnetic field is applied. The observation of this effect is a method to find new singlet fission materials.
We found new perylenediimides (PDIs) with different functional groups to undergo the singlet fission process. The molecular packing of the different PDIs affects the way how the singlet fission efficiency behaves at different magnetic field strengths.
Attaching a singlet fission material to a conventional solar cell material can cause a transfer of excitons from the organic to the inorganic semiconductor and therefore lead to high efficiencies of hybrid solar cells.
By investigating whether excitons can transfer from the singlet fission material tetracene into a solar cell material in a bilayer system, we found that there is an interaction between both layers. The photoluminescence intensity of the solar cell material correlates with the amount of singlet excitons in the tetracene. This can be explained by either exciton transfer or photon transfer.

Contents

Abbreviations

Al_2O_3: Aluminum oxide

ALD: Atomic layer deposition

DCT: direct charge transfer

DET: Dexter energy transfer

DPH: Diphenylhexatriene

FA: Formamidinium

HOMO: Highest occupied molecular orbital

InGaAs: Indium gallium arsenide

LP-filter: Longpass filter

LUMO: Lowest unoccupied molecular orbital

MA: Methylammonium

MFE: Magnetic field effect

PDI: Perylenediimide

PL: Photoluminescence

PV: Photovoltaics

PRV: Low bandgap perovskite

SQ-limit: Shockley-Queisser-limit

Tc: Tetracene

TTA: Triplet-triplet annihilation

1 Introduction & Background

The world's increasing population and prosperity both lead to an increasing demand of energy worldwide.[16] The market for generation of energy has always been dominated by the use of fossil fuels which is the main reason for the man-made emission of carbon dioxide (CO_2), the greenhouse gas which is leading to an increase of global temperature. To counteract the global warming, more people than ever call on society and on governments to act to protect nature, reaching its preliminary peak with the third global climate strike in September 2019.
To reduce CO_2 emissions, renewable energy sources like wind and solar power gain popularity. Especially photovoltaics (PV) are promised to have a big market share in the future since, on human timescales, the sun is an unlimited source of energy. Low costs and high efficiencies of solar cells are crucial to increase their economic viability.
However conventional solar cell efficiencies are limited by the so-called Shockley-Queisser limit (SQ-limit) of 33.7% [21],[19] which is almost reached by current research solar cells.[7],[28] A main reason for efficiency loss in the SQ-limit calculation is that a large part of the solar spectrum cannot be used optimally: If the energy of incident light is too low, photons will not be absorbed by the solar cell. If the energy is too high, only a part of it can be used to create electricity.

One approach to reach efficiencies beyond the SQ-limit is singlet exciton fission (singlet fission). In some organic materials that perform the singlet fission process, one incident photon with high energy can excite not only one pair of charge carriers with an energy too large for a conventional solar cell, but two pairs with each half the energy. Attaching a singlet fission material to a conventional solar cell could prevent a large efficiency loss, by using high energy photons more effectively to create two pairs of charge carriers instead of one. These charge carriers can then be used for generating electricity.

In this thesis a class of materials (perylendiimides) is examined to see whether some molecule types undergo the singlet fission process. Also it is investigated whether energy can be transferred from the singlet fission material tetracene to a solar cell material, which would enable highly efficient hybrid solar cells.

1.1 Working principle of a solar cell

The basic concept of a solar cell is the conversion of light into electricity. This happens because a photon can excite an electron into a higher energy state. In semiconductors the electron is excited from the valence band into the energetically higher conduction band, which are separated by at least a certain energy gap, called the bandgap. This is the minimum amount of energy a photon is required to have to excite an electron. By being excited into the conduction band the electron is leaving a vacancy behind in the valence band. This absence of an electron is referred to as hole and is acting as a counterpart of the electron. Together they form an electron-hole pair. After being excited by a photon with a certain amount of energy, the electron will relax back into the lowest energy state of the conduction band. Meanwhile the hole in contrast will move to the highest energy level in the valence band so electron and hole will be separated by the bandgap energy. The difference between the excitation energy from the photon to the bandgap energy is thermally dissipated. The latter process is called thermalization and is one of the main reasons of efficiency loss in solar cells because the energy dissipated cannot be used to generate a current.
In order to use these charge carriers to power an electrical load they need to be separated. The separation normally happens via a p-n junction which leads to electrons moving to the p-doped region and holes moving to the n-doped region. This creates an internal voltage in the solar cell. The generation of charge carriers by incident photons then causes an electric current. By contacting both the ends of the p-n junction, electrons can run through an electrical load to the p-side where they can recombine with the holes again.

1.2 Shockley-Queisser-Limit

In 1961 W. Shockley and H.-J. Queisser calculated a limit in power conversion efficiency that single junction solar cells could not overcome. They predicted that a maximum efficiency of 30% could be

achieved by a semiconductor with a bandgap of $E_g = 1.1\,\text{eV}$[21]. This was later expanded to an efficiency of 33.7% at a bandgap of $E_g = 1.34\,\text{eV}$[19]. According to SHOCKLEY and QUEISSER the limit in efficiency of single junction solar cells is mainly dependent on three effects:
Every material with a temperature above 0 K sends out thermal radiation which is known as **blackbody radiation**. A certain amount of the energy that the solar cell is absorbing from the solar radiation will be emitted by thermal radiation.
Another reason for the limit is **charge recombination**. As the irradiation of a solar cell leads to creation of an electron-hole pair, the reverse process is happening as well: Electron-hole pairs recombine radiatively and send out a photon. In the end this leads to a loss of efficiency of the solar cell because the electron and hole involved cannot be separated and used for current generation.
A very important factor for the SQ-limit is the **spectrum losses**. For incident light with $E_\nu = E_g$ all the energy of a photon is put into the creation of an electron-hole pair. As mentioned above, the bandgap energy E_g of a semiconductor used for a solar cell is an important criterion for the efficiency. Incident photons with an energy $E_\nu < E_g$ cannot excite an electron into the conductance band and will therefore not be absorbed. For the efficiency of the solar cell they are 'lost'. An incoming photon with $E_\nu > E_g$ will transfer all its energy to an electron, by exciting it into the conduction band. The electron will lose all the excess energy above the band edge by sending out phonons, which is referred to as thermalization.

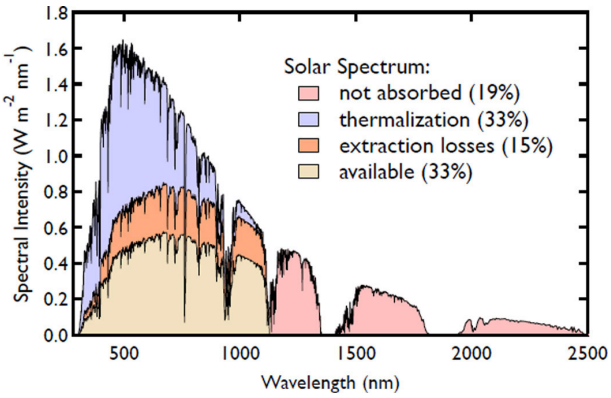

Figure 1: Schematic view of different types of efficiency losses in a silicon solar cell shown as part of a solar spectrum: Photons with less energy than the bandgap are not absorbed (rose). The angular dependent extraction of blackbody radiation resulting in charge carrier recombination is referred to as extraction losses (orange). Excited electrons created by high energy photons lose their excess energy via thermalization (blue). What remains is the beige part which can create charge carriers leading to a maximum efficiency of 33%.[20]

1.3 Singlet Fission

In organic semiconductors there is no concept of a valence and conduction band. Different energy states of electrons are given by the fact that each molecule has several molecular orbitals with different energy levels occupied by at most two electrons each. In these materials an incident photon can excite an electron from the highest occupied molecular orbital (HOMO) into the lowest unoccupied molecular orbital (LUMO). The result is the first excited singlet state S_1. It is a bound electron-hole pair which is referred to as exciton.

One attempt to reach efficiencies beyond the SQ-limit is to use the singlet exciton fission process (or just singlet fission (SF)). The goal is to reduce thermalization losses. The basic idea of singlet fission is that a high-energy photon (green and blue light) will create not only one exciton with high energy but two excitons with each half the energy. Singlet fission is a process which occurs in some organic semiconductors. If such a singlet fission material could be attached to a conventional solar cell, these excitons could be transferred to the solar cell, dissociating into electron-hole pairs. Because one high-energy photon leads to two electron-hole pairs in the end, a certain amount of thermalization would be prevented and the efficiency of the solar cell increased.

1.3.1 The Singlet Fission Process

By the absorption of a high energy photon in an organic semiconductor, an electron is excited from the HOMO into the LUMO resulting in an excited singlet state exciton S_1. In singlet fission materials the S_1 state can 'share' its energy with an unexcited neighboring molecule in the ground state S_0. The result is the formation of two spin triplet states T_1, each with roughly half the energy of S_1. A spin singlet state corresponds to the spin quantum number 0, while a triplet state's spin number is 1. The singlet fission process is spin allowed because of the formation of an intermediate state of a correlated triplet pair $^1(TT)$. The $^1(TT)$ state, consisting of two triplet excitons has the overall spin 0 so transitions from S_1 to $^1(TT)$ are spin allowed because the overall spin is conserved. The correlated triplet pair can be seen as a combination of two triplet states. Its wave function can be interpreted as a coherent superposition of the wave functions of the nine sublevels that result from the combination of two triplets.[1] The singlet fission process from the excited singlet states to the triplets via a correlated triplet pair can be written schematically as in equation (1) in a simplified way.[8],[1]

$$S_0 + S_1 \underset{k_2}{\overset{k_{-2}}{\rightleftarrows}} {}^1(TT) \underset{k_1}{\overset{k_{-1}}{\rightleftarrows}} T_1 + T_1 \tag{1}$$

Both steps, either the formation of a triplet pair from the initial excited singlet state plus the ground state, and the formation of two separated triplets from a $^1(TT)$ pair, can also occur in the opposite direction. The interconversion between the initial $S_0 + S_1$ state and the correlated triplet pair $^1(TT)$ is described by the two rate constants k_{-2} and k_2. The interconversion between the triplet pair and the two separate triplets T_1 is described by k_{-1} and k_1. The whole process starting with a ground state and an excited singlet state into two separated triplets is called singlet fission. The reverse process is the formation of an exited singlet state out of two free triplets. This process is called triplet fusion or triplet-triplet annihilation (TTA).
The different rate constants (k_x) heavily affect the equilibrium of excited singlet states S_1 and triplets T_1 in a singlet fission material. In singlet fission materials like tetracene or pentacene the efficiency of the singlet fission process is very high, therefore a large fraction of singlet excitons is converted into triplet excitons via the singlet fission process[1]. One could say that the rate constants k_{-1} and k_{-2} outcompete the rates k_1 and k_2. The singlet fission process in tetracene for example happens on timescales $\ll 1\,\mu s$[14] while the triplet lifetimes are around $100\,\mu s$[25]. Exciting a singlet fission material like tetracene leads to a large number of excited T_1 states compared to a small number of excited S_1 states.

1.3.2 Transfer of Excitons

In order to harvest the triplet excitons generated by the singlet fission process for a solar cell, the excitons must migrate to the solar cell material. The triplets can move from molecule to molecule via Dexter energy transfer (DET). In the concept of DET one excited electron of the donor molecule is exchanged with a ground state electron of the acceptor molecule (see fig. 2). In order for DET to happen the wave functions of the two molecules must overlap which means that distances between donor and acceptor molecule must be small (typically in the order of about few nanometres).[2]

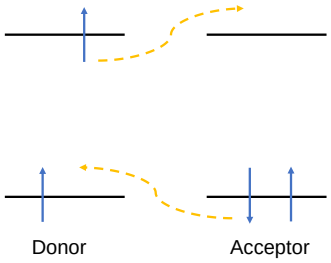

Figure 2: Schematic depiction of Dexter energy transfer of an excited triplet state. The excited electron from the donor is exchanged with an electron in the ground state of the acceptor.[27]

The long lifetimes and diffusion lengths of the triplets in tetracene[25] make it possible that they can actually reach the solar cell material. The transfer from the SF material to the semiconductor (silicon or perovskite) can also happen via DET. So the whole triplet exciton is transferred to the solar cell material. But in the crystalline structures of silicon or perovskite the binding energies of the excitons are way smaller than in organic semiconductors.[5],[15],[10] That is why excitons in silicon or perovskite will dissociate quickly into electron-hole pairs. In order of DET to happen at the interface between the SF material and the inorganic semiconductor the wave functions of the different molecule types must overlap which to the best of our knowledge has not been shown yet.
When the triplet excitons are transferred and dissociated into electron-hole pairs in the solar cell material, the charge carriers can be separated and used for current generation.
If they are not separated, some of them will recombine radiatively sending out photons with about the energy of the bandgap. This radiative recombination is called photoluminescence (PL). Also the excited singlet exciton S_1 can recombine radiatively sending out photons with the respective energy $E(S_1)$. The triplet excitons T_1 show no PL because the transition of the excited electron to the ground state would be spin forbidden according to PAULI's exclusion principle. In figure 3 there is given a schematic view of the singlet fission process resulting in triplet excitons transferring into a solar cell material and dissociating into electron-hole pairs.

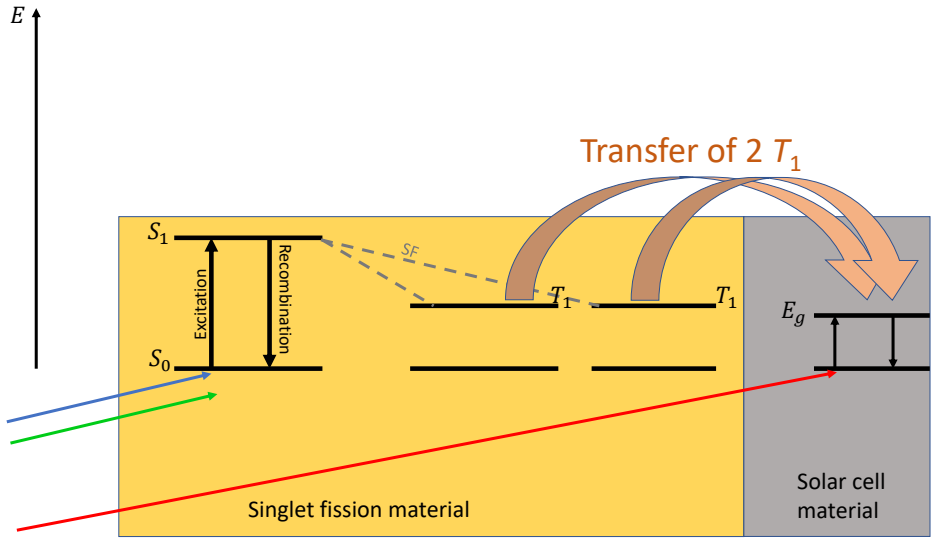

Figure 3: Schematic view of a SF–solar cell material bilayer sample. The high energy photons (blue and green light) are absorbed in the SF material and excite singlet excitons S_1. Through the SF process, the singlet converts into two triplet excitons. These can move via DEXTER energy transfer towards the solar cell material. When they transfer into the low bandgap semiconductor they dissociate into electron-hole pairs which can be used for generating a current in a proper device. The red photons have too little energy to be absorbed by the SF material. They are transmitted and finally absorbed by the solar cell material creating electron-hole pairs. Both the singlet exciton in the SF material and the electron-hole pair in the low bandgap semiconductor can recombine radiatively again. By that, photons are emitted with the respective energy which is referred to as photoluminescence (PL). The triplet excitons can not recombine since the transition to the ground state is spin forbidden.

1.3.3 Magnetic Field Effects

In the late 1960s R. C. JOHNSON and R. E. MERRIFIELD found that the behavior of triplet and singlet excitons in a SF material changes when an external magnetic field is applied.[8] They investigated crystals of the SF material anthracene and found that the intensity of the delayed fluorescence (DF) would increase at low magnetic fields reaching its maximum at B = 0.035 T and it would decrease at high B-fields reaching a saturation at around B = 0.5 T. 'Delayed fluorescence' is the PL of the S_1 state. But not the radiative recombination after excitation (which is called 'prompt fluorescence' (PF)). DF is the PL of excited singlets formed by triplet-triplet annihilation. This DF occurs later than the PF because at

least one SF process must have happened before the recombination. In contrast, the prompt fluorescence intensity behaves in the opposite direction when a B-field is applied: first it decreases at low fields and then increases again in a strong B-field. A schematic behavior of the prompt and delayed fluorescence in an external magnetic field is shown in figure 4.

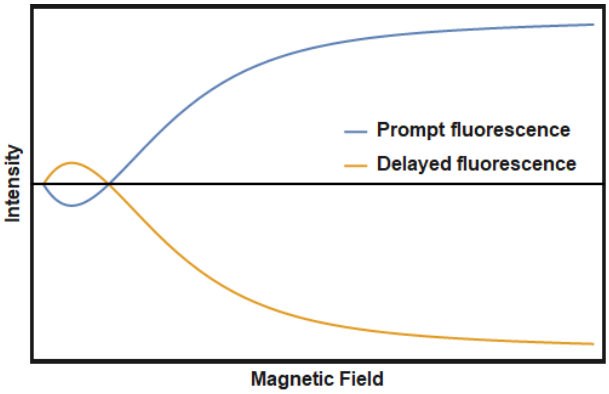

Figure 4: Scheme of the behavior of prompt (blue) and delayed (orange) fluorescence intensity in an external magnetic field. Figure adapted from M.B. Smith & J. Michl. [1]

The intensity of prompt and delayed fluorescence corresponds indirectly to the amount of excited singlets S_1 (prompt) and excited triplets T_1 (delayed) in the material after an excitation: when there are more singlets in the material after an excitation the prompt fluorescence will be stronger. When the amount of triplets is high, the delayed fluorescence intensity will be high as well. This is why the blue and orange curve in figure 4 will be referred to as 'singlet curve' (blue) and 'triplet curve' (orange) below in this thesis.
In figure 4 we can see, that in low magnetic fields there are more excited triplets in the material and in high magnetic fields the amount of singlets is increased. It has to be said that the amounts of the different types of excitons are not compared to each other. They have to be compared to the respective amount when there is no magnetic field. So at high B-fields the singlet amount is higher compared to when there is no magnetic field. In total, the singlet fission efficiency in the materials like tetracene is still very high as mentioned in chapter 1.3.1. So we assume that even in strong B-fields the number of triplet excitons is way larger than the number of singlet excitons.
The fact that the amounts of excited singlets and triplets in the material change if a magnetic field is applied, indicates that the efficiencies of singlet fission and triplet-triplet annihilation are affected by the B-field. By having a look at equation (1) again

$$S_0 + S_1 \underset{k_2}{\overset{k_{-2}}{\rightleftarrows}} {}^1(TT) \underset{k_1}{\overset{k_{-1}}{\rightleftarrows}} T_1 + T_1,$$

we find that the rate constants k_x change in an external B-field. So since there are more singlets when the B-field is strong, the rates k_1 and/or k_2 will increase or the rates k_{-1} and/or k_{-2} will decrease. So the equilibrium of S_1 and T_1 will shift towards the left hand side of the equation. The opposite is the case at low magnetic fields.
The change of the rate constants shifting the equilibrium towards triplets in low B-fields is explained by an enhancement of the interaction between the nine spin sublevels in the correlated triplet pair ${}^1(TT)$.[1],[26] By enhancing the interaction of these sublevels the formation from a singlet spin state with spin quantum number 0 to two triplet spin states with spin quantum number 1 (happening in the correlated triplet pair) is facilitated. One could interpret this as an increase of the rate constant k_{-1} resulting in more triplet excitons. While correlated triplet pairs convert easier to separated triplets the number of singlets formed from ${}^1(TT)$s will decrease resulting in a decrease of rate constant k_2.
If the B-field is increased further, the Zeeman splitting occurs. At strong magnetic fields the energies of the spin sublevels of the correlated triplet pair are split up and so do not match as well as before. The

formation from a spin singlet state to two spin triplet states is hindered by this. In equation (1) this can be interpreted as a decrease of k_{-1} and so there are more correlated triplet pairs converted into singlet excitons resulting in an increase of k_2. The equilibrium shifts towards more singlets at strong B-fields.

By continuously exciting a singlet fission material, the PL - caused by excited singlets recombining - can be measured. As mentioned above, the amount of singlets which lead to a PL, changes when a magnetic field is applied. That is why the blue singlet curve in figure 4 can also be seen as a change in intensity of the PL when a B-field is applied. It turns out that measuring the PL intensity while an external B-field is applied, is a method to check whether a material undergoes singlet fission. The PL intensity will then have the shape of the singlet curve.

However, the amount of triplets in an external B-field will change in shape of the orange triplet curve in figure 4. One part of this thesis will investigate whether triplet excitons transfer from a singlet fission material into a solar cell material. If they do, the number of excited electron-hole pairs in the semiconductor will be correlated to the number of triplets formed by the SF material. It will be correlated to the triplet amount (and not to the singlet amount) because of the high SF efficiencies mentioned above, causing more triplets to be involved than singlets. Measuring the PL intensity of the solar cell material caused by e-h pairs, will provide evidence for exciton transfer, if a triplet curve is observed.

1.3.4 Materials

In this thesis the methods of using an external magnetic field, described in the previous paragraph, will be used to investigate the singlet fission behavior of different molecules of perylendiimides and to examine whether triplets transfer from the SF material to a low bandgap semiconductor.

Perylenediimide is a molecular structure consisting of perylene (five benzene rings ($C_{20}H_{12}$)) with an imide group at each end (two acyl groups bound to nitrogen). Polycrystalline thin films of slip-stacked PDIs have been found to perform singlet exciton fission.[3] That is why we investigate thin films of PDI molecules where functional groups are added either at the acyl group or in the so called bay-area (left and right hand side of the perylene part). It should be found out by that, whether adding different functional groups enhances the singlet fission efficiency. The ultimate goal is to find new singlet fission materials and to achieve a better knowledge about which molecular structures and packings in general are favourable to do singlet fission.
The particular molecules which were used in this thesis are depicted in figure 5.

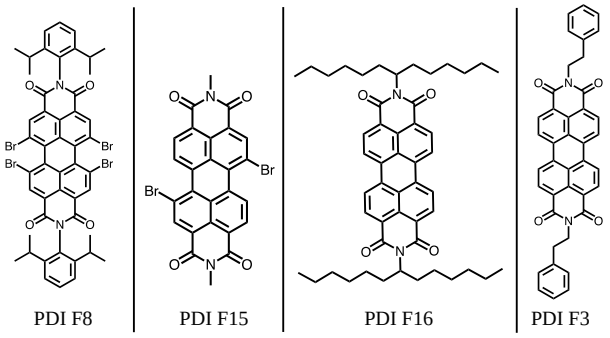

Figure 5: Molecule structures of the different PDIs investigated in this thesis. For results see chapter 2.2, figures 15, 16, 17, 18 respectively.

In the other part of the experiment in this thesis we want to examine whether triplet excitons will transfer from the singlet fission material **tetracene** into a low bandgap semiconductor.
Polyacenes like anthracene, tetracene, pentacene, hexacene are found to perform the singlet fission process already in the late 1960s[1]. They consist of a linear aligning of benzene rings, each as many as stated in the molecule name. So the structure of tetracene, for example, looks like it is shown in figure 7. At room temperature tetracene forms an orange powder (see fig. 6). It can be thermally evaporated forming thin films.

Figure 6: Tetracene in powder form.[22]

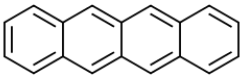

Figure 7: Molecular structure of tetracene. Four benzene rings in a straight alignment.[22]

The excitation energy of a singlet exciton in tetracene is $E(S_1) = 2.32\,\text{eV}$[23] which leads to a PL peak at 540 nm when singlets are recombining radiatively (see fig. 19 for a measured PL spectrum of tetracene). The triplet energy in tetracene is $E(T_1) = 1.25\,\text{eV}$. What stands out by comparing both energies is that twice the triplet energy exceeds the singlet energy such that $E(S_1) < 2E(T_1)$. It is remarkable that the singlet fission efficiency in tetracene is very high even though it seems that the energy difference $2E(T_1) - E(S_1) > 0$ does not favor the process. An explanation for SF to happen anyway is given by a gain of entropy during the conversion of two triplet excitons out of a singlet. More specific: the entropy is gained in the step of generating two separated triplets $T_1 + T_1$ out of the correlated triplet-triplet pair $^1(TT)$. While the $^1(TT)$ state is localized on two molecules of the delocalized initial singlet exciton which has a larger spatial extent. The separation of the triplets occurs when one triplet exciton hops onto another molecule outside the initial singlet state. A schematic view of the states and their spatial extent is depicted in figure 8.

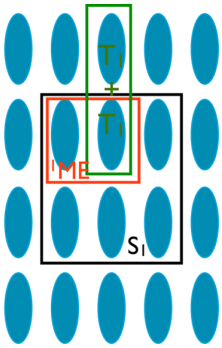

Figure 8: Schematic image of the spatial extent of the different states involved in the SF process. The singlet S_1 (black square) is delocalized over several molecules. The triplet pair $^1(TT)$ (here: multiexciton ^{1}ME) (red) is localized on two adjacent molecules of the initial singlet. If a triplet hops onto another molecule, the pair becomes separated into two T_1s (green). Figure adapted from Kolomeisky, Feng & Krylov.[11]

While the $^1(TT)$ state is localized in the borders of the initial singlet state, there are more possibilities for two separated triplets to occur. This is where the gain of entropy shows up. If the gain of entropy outcompetes the energy difference between one excited singlet and two separated triplets, the Gibbs free energy G will decrease. In systems with a constant pressure and temperature thermodynamic processes will go for a minimum of G ($\Delta G \leq 0$). A more detailed explanation of the thermodynamic model can be found in reference [11].

1.4 Perovskites

In recent years perovskites have gained major attention by the research field of photovoltaics. The term *perovskite* basically describes a typical crystal structure which is depicted in figure 9. The interest in photovoltaics mainly lies in the metal halide perovskites where for the substitute B a metal (usually lead or tin) and for X a halide is used. These metal halide perovskites are semiconductors whose bandgap energies can be tuned by using different components for the substitutes A, B, X.[6],[13] Research progress in perovskite solar cells is developing relatively fast. State of the art perovskite solar cells reach efficiencies up to 25,2%.[17] A use of the material class is also attractive because the fabrication is relatively easy and cheap. They can be fabricated out of solutions by spin coating and evaporating.

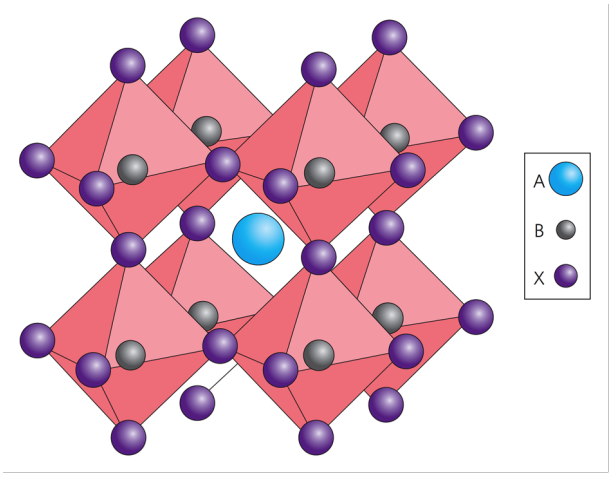

Figure 9: Perovskite structure. In the experimental part of this thesis A is substituted by either FA or MA, B is substituted by lead or tin and for X Iodine is used: $(FASnI_3)_{0,6}(MAPbI_3)_{0,4}$. Figure adapted from M. A. Green *et al.*[6]

With $(FASnI_3)_{0,6}(MAPbI_3)_{0,4}$[24] a perovskite is found whose bandgap of $E_g = 1.25\,\text{eV}$ matches the energy of a triplet exciton in tetracene. This could allow triplets to transfer from Tc into the perovskite when a Tc-PRV bilayer is used.

2 Experiment

The experiment that we use to investigate whether a material does singlet fission takes advantage of the photoluminescence (PL) of the material sample. By varying the strength of an external magnetic field we examine whether the intensity of the PL is changing. If the amounts of excited singlet excitons and triplet excitons behave as described in chapter 1.3.3, the PL intensity will change in the same way. This would be a strong indication for the material to do singlet fission.

2.1 Experimental setup

To observe the magnetic field effects the sample is placed between two magnetic coils. A laser diode excites a spot on the surface of the sample. A photodetector is measuring the intensity of the resulting PL. (See figures 11 and 12 for a photo and a scheme of the setup.)
To protect the samples from contamination and reaction with oxygen they are all stored in a nitrogen atmosphere. If they are needed for the experiment they are encapsulated in air tight quadratic boxes made of stainless steel with a glass window which is glued on top (see fig. 10).

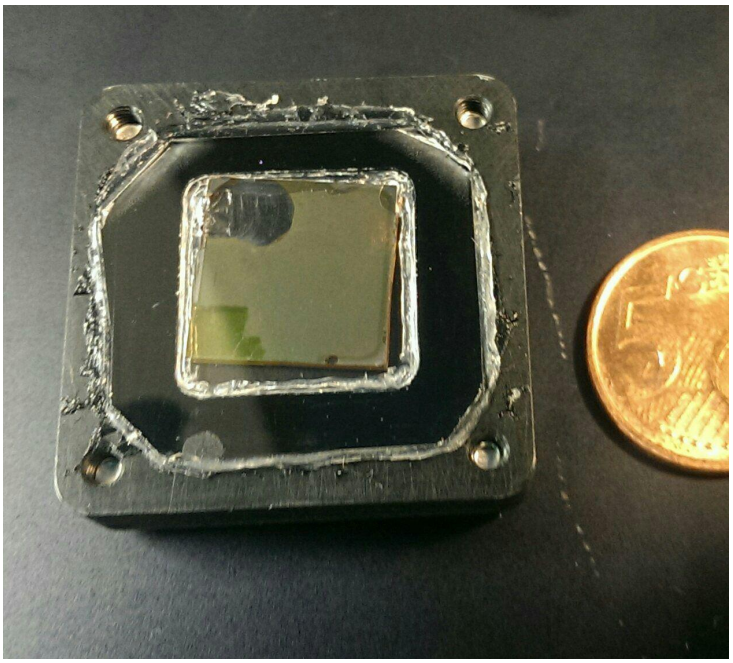

Figure 10: Encapsulation: a sample of Tetracene on top of low bandgap perovskite encapsulated in a frame of stainless steel covered by a glass plate which is glued on top.

The electromagnet is the model `3470`, provided by `GMW Magnet Systems` and can create a magnetic field with a flux density up to $B_{max} = 0.5\,T$. To avoid any movement in the setup during the measurement the sample holder is clamped down with screws on an optical table.
Two lenses focus the PL onto the photodetector. For the detection either a silicon diode or an InGaAs diode is used. They can also be exchanged with an attachment for an InGaAs spectrometer (model `SP-2300i` from `Princeton Instruments`). The photodetector's output signal is sent to a lock-in amplifier (`Stanford Research Systems`, model `SR830DSP`) which also drives an optical chopping wheel that is placed in front of the laser. By connecting both the chopping wheel and the detector to it, the lock-in amplifier is used to remove noise coming from ambient light and other sources.
We use a continuous `L520P50` laser of 520 nm wavelength in a `TCLDM9` laser mount, both purchased by `ThorLabs`. By focusing the laser on a very small spot on the sample we reach excitation densities up to $1.0\,\frac{kW}{cm^2}$. A part of the laser light will be reflected at the glass surface which is protecting the sample from air. To prevent detecting that reflection in the output signal we use a 550 nm longpass filter which transmits only wavelengths above 550 nm. Additional filters can be added which can be useful to distinguish which material emits the PL when investigating a bilayer.

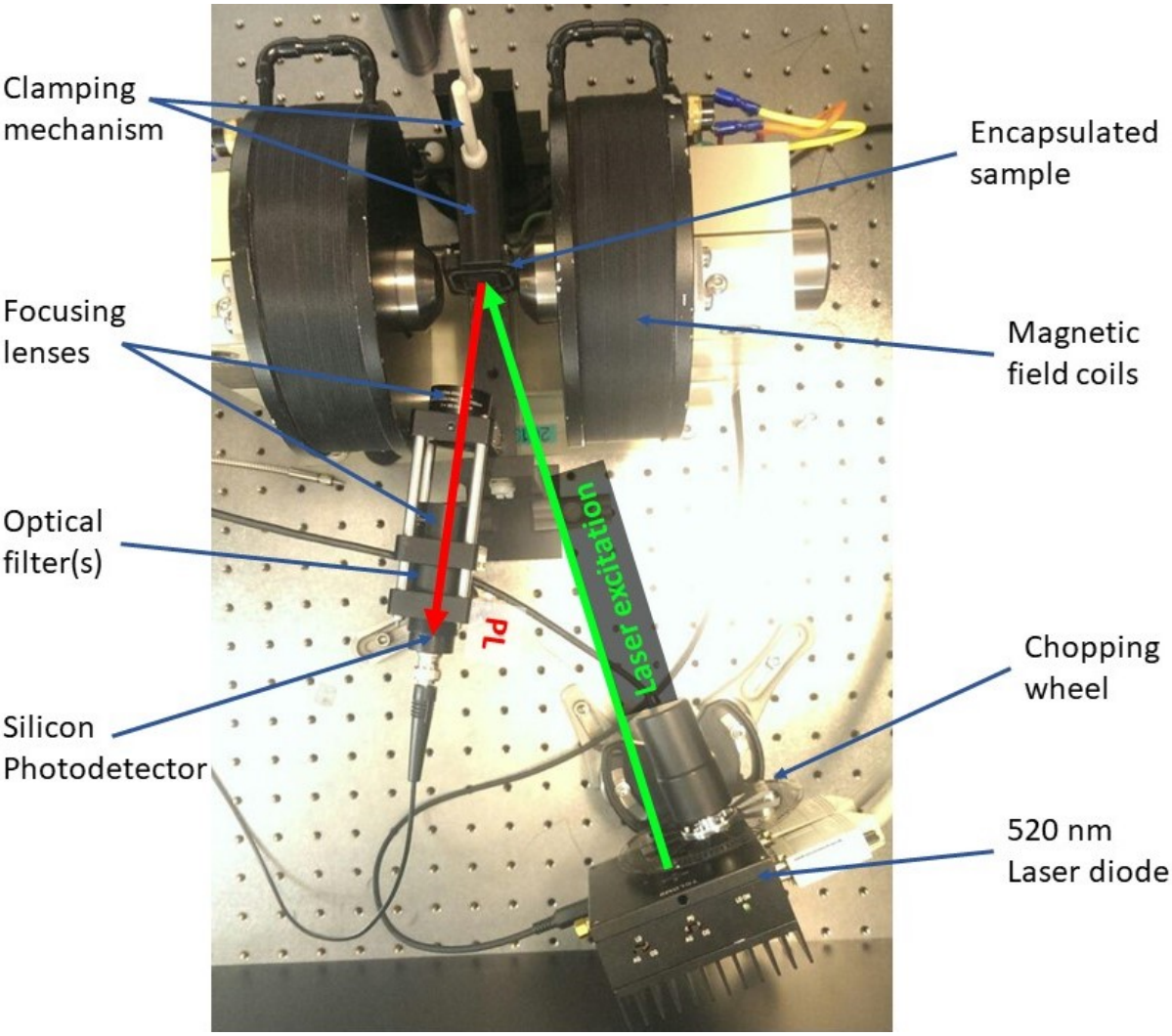

Figure 11: Experimental setup

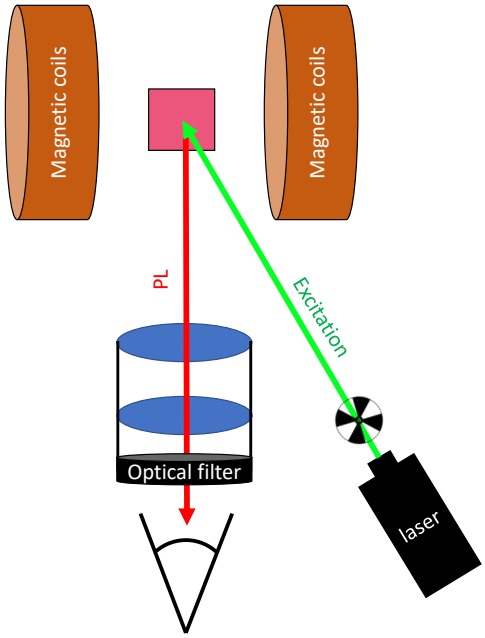

Figure 12: Setup scheme: A 520 nm laser excites the sample standing between the magnetic field coils. The resulting PL is focused and passes an optical filter before reaching the photodetector.

2.2 Perylene diimides (PDIs)

In the first case the materials to investigate are thin films of different molecules of PDI on a glass substrate. The different films have thicknesses from 50 nm up to 500 nm. The goal is to find materials that go through the singlet fission process. Therefore the setup described in chapter 2.1 is used.
The samples are constantly illuminated by a 520 nm laser. Meanwhile the magnetic field strength will be increased stepwise. After every step the intensity of the PL of the sample is measured by the photodetector. If the magnetic field effects - described in chapter 1.3.3 - occur, the PL intensity should also change in a shape such as in figure 4 when the external B-field is being increased.
To quantify how much the PL intensity changes in the B-field, the intensities $I(\mathrm{B}_x)$ of the respective measuring step x are each subtracted by the PL intensity value without a magnetic field $I(\mathrm{B}=0)$ (magnet turned off) and then divided by $I(\mathrm{B}=0)$. The resulting value describes how much the PL changed at a certain B-field strength compared to the sample's PL without an external magnetic field.

$$\text{PL change}(\mathrm{B}) = \frac{I(\mathrm{B}) - I(\mathrm{B}=0)}{I(\mathrm{B}=0)} \tag{2}$$

By illuminating the sample with high laser powers the substances seem to degrade such that the PL intensity decreases more the longer the excitation. This means that in the end of a measurement (which takes from two up to ten minutes) the PL intensity can be way lower than in the beginning. A comparison of intensities is made more difficult by that: By the constant illumination and the degradation involved, the value of $I(0)$ will change over time and will become lower at the end of the measurement. The resulting calculations of the change in the PL intensities would be falsified if the same value for $I(0)$ is used in every step. To be able to calculate the PL change anyway we used a certain sequence of measurement: After every step of increasing the field strength and measuring the PL, the magnet is turned off again and a new value for $I(0)$ is measured. The value for the PL intensity change can then be calculated like in equation (2) with a new $I(0)$ for every different B. In figure 13 it is depicted how the magnetic field is increased during one measurement. The current flowing though the coils is synchronized with the time of each intensity measurement step.

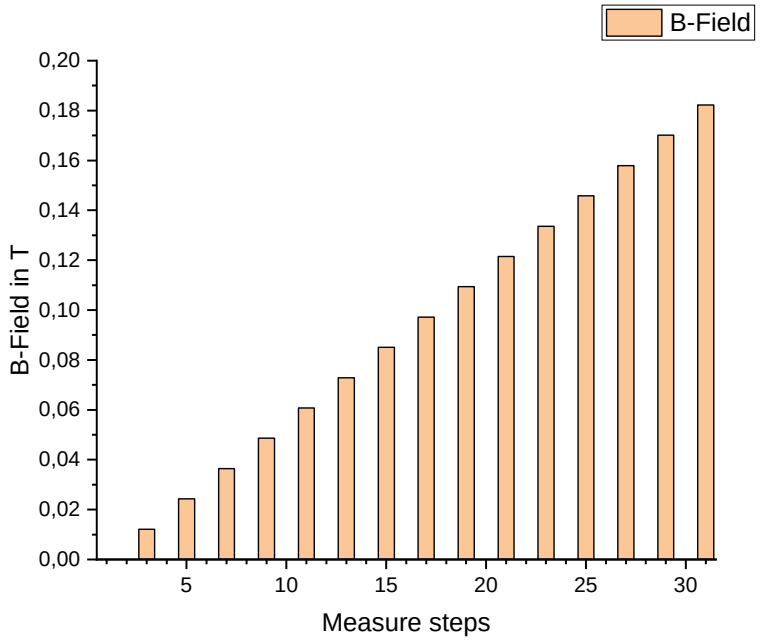

Figure 13: To be able to calculate the change in the PL intensities despite the degradation of the sample, the magnet is turned off after every measuring step and a new value for $I(0)$ is measured. The change of PL intensity compared to B = 0 is then calculated by $\frac{I(\text{step}x)-I(\text{step}(x-1))}{I(\text{step}(x-1))}$ while at step x the magnet is turned on.

Figure 14 shows how the intensity of the PL of sample PDI F8 changes when the magnet is turned on and off alternately. The further the measurement progresses, the higher the magnetic field strengths become. You can clearly see the overall downwards trend of intensity which is caused by the degradation of the sample. The changes of the intensities caused by the magnet which are shaped like spikes in figure 14 are way smaller than the loss of intensity coming from the degradation. That is why it is so important to remeasure $I(0)$ after every step.

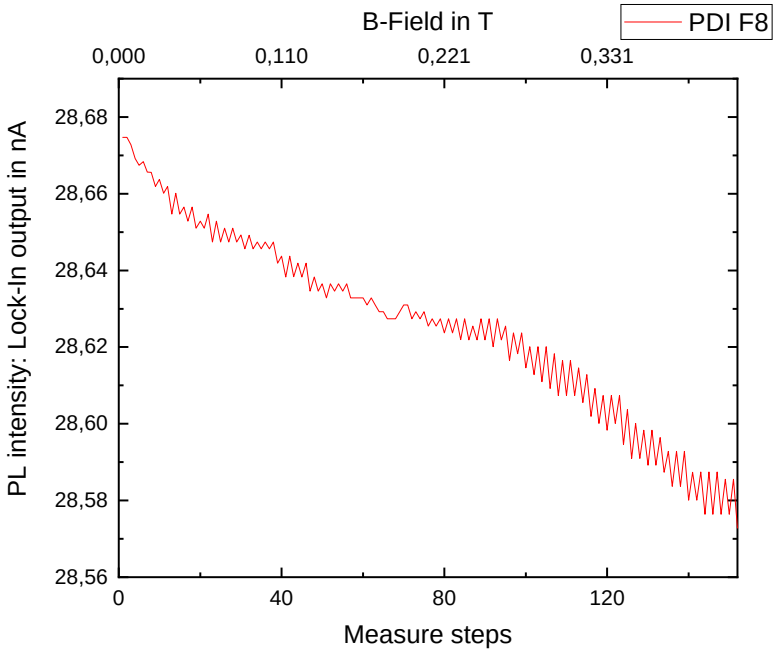

Figure 14: Photoluminescence intensity of a PDI F8 sample changing at different measuring steps. Every second step represents a different magnetic flux density from the external field. In the steps in between the intensity at B = 0 is measured to calculate the PL change as in equation (2).
The output current from the Si-photodetector via the lock-in amplifier is depicted on the y-axis.

The spikes in the last few steps of the measurement are bigger than they are in the beginning. This indicates that a stronger magnetic field causes a greater change in PL intensity. Also, there is a region between steps 60 and 65 where the magnetic field doesn't seem to have a strong impact on the PL since there are no clear spikes visible.
To better analyze the measurement and focus on the PL changes we now calculate the change in intensity dependent on the strength of the magnetic field by using equation (2). Now the $I(0)$ values are only used for the calculation but are not shown graphically. The result can be seen in figure 15.

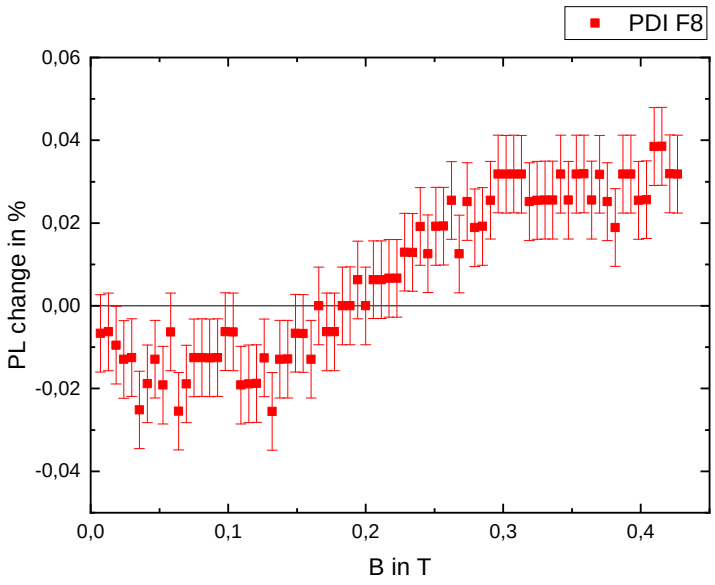

Figure 15: Sample of PDI F8: Change of PL intensity in an external magnetic field calculated as described in formula (2). The error bars are calculated via the combined uncertainty according to equation (2). Therefore the uncertainty of the lock-in output was used which was assumed to be the standard deviation of the signal, when no magnetic field was applied.

In figure 15 it is shown that by increasing an external magnetic field the PL intensity of this sample first becomes up to 0.02% lower until B = 0.1 T. At B = 0.2 T it is again equal compared to the PL without a magnetic field. By increasing B further the PL signal becomes stronger again until a saturation of 0.03% more (compared to B = 0) at B = 0.3 T.

A similar result is seen in figure 16 with the results of the same experiment with a sample of PDI F15. But even if the shape of the curves in figures 15 and 16 looks similar there are some quantitative differences. The strength of the magnetic field where the curve changes its sign from minus to plus is shifted to a smaller value of B. It is now rather at B = 0.15 T. With regard to the uncertainties it can not be made clear whether the saturation point is also shifted to a smaller B. What is striking, however, is that the amount of change in the PL is about one order of magnitude greater than it was in the attempt with the PDI F8 in figure 15. Now it reaches up to 0.4% at a magnetic field of B = 0.4 T.

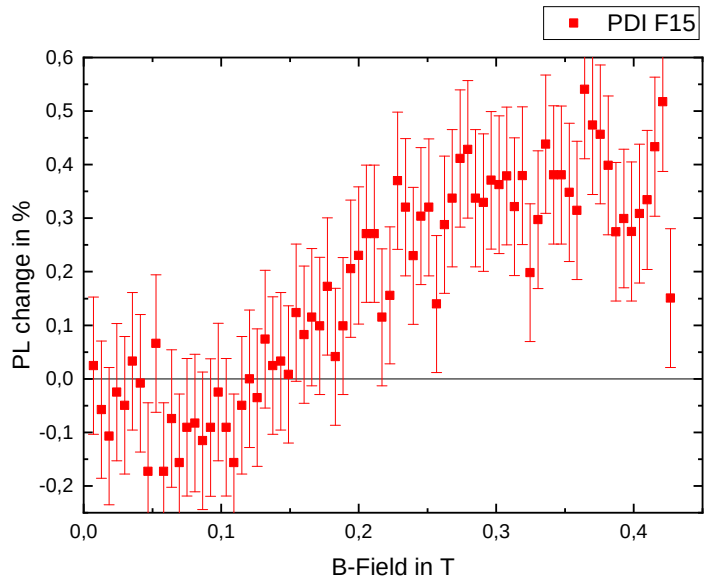

Figure 16: Sample of PDI F15: Change of PL intensity in an external magnetic field.

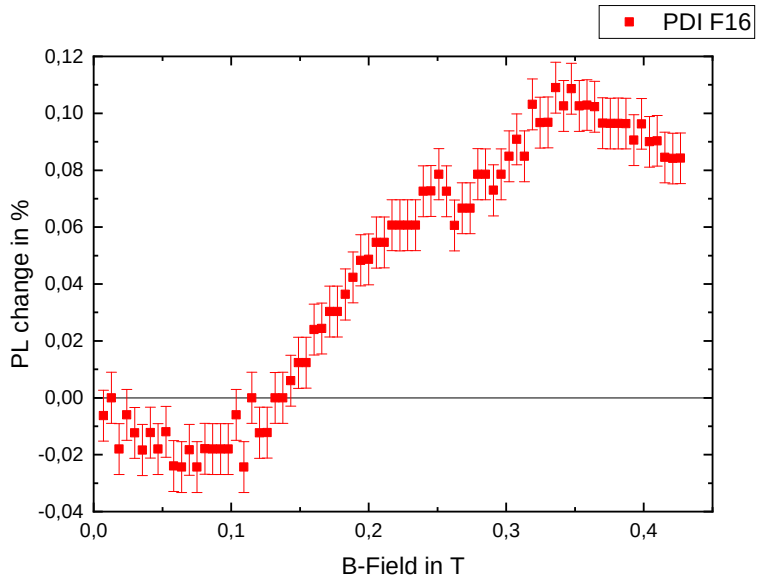

Figure 17: Sample of PDI F16: Change of PL intensity in an external magnetic field.

The result of PDI F16 in figure 17 shows the shape of the curve as well. There is also the negative bump at $B = 0.075\,T$ and the change of sign at $B = 0.15\,T$. These values are rather comparable to those form PDI F15 in figure 16 than to those of PDI F8 in figure 15. The relative change in the PL intensity of PDI F16 reaches up to 0.1%.

Looking at the results of the PL changes in an external magnetic field of the PDI samples F8, F15 and F16, they all have the shape of the singlet curve which was shown in figure 4. This is a strong indication that singlet fission happens in these particular materials. What stands out when comparing the results in the figures 15, 16 and 17 is that the curves of PDI F15 and PDI F16 are shifted to smaller

magnetic fields compared to the curve of PDI F8. The change in sign from minus to plus in the latter is at 0.2 T while in the results of F15 and F16 it is at 0.15 T. Also striking is the difference in the relative PL change values. The maximum change goes from 0.03% (PDI F8) over 0.1% (PDI F16) up to 0.4% (PDI F15). These differences could be explained by a different packing of the molecules in the film. In the publication of M. Wakasa *et al.*[26] it is found that the packing of the molecules of the SF material diphenylhexatriene (DPH) plays a significant role on the PL behavior in a B-field. It is distinguished between several parallel packing structures, tilted alignments or herringbone structures (zigzag patterns). Each different molecule alignment type leads to a different behavior of the PL in a B-field. This also affects the efficiency of singlet fission which could explain why the maximum PL change values differ in our PDI results. The reason for the different behavior is explained by the various diffusion paths of the correlated triplet pairs in the different packing patterns. Each diffusion pathway leads to another rate constant k_{-1} for the generation of separated triplet excitons.
It could well be that the investigated PDIs in this thesis also have varying molecular packing structures that lead to the different behavior in external B-fields. At the moment the molecular packing of these samples is unknown.

The fourth molecule, PDI F3, whose PL was also investigated in an external B-field showed a result which was different from the first three samples seen above. The change in PL intensity was not shaped like the singlet curve but basically flipped at the 0% line resulting in a triplet curve (see figure 18).

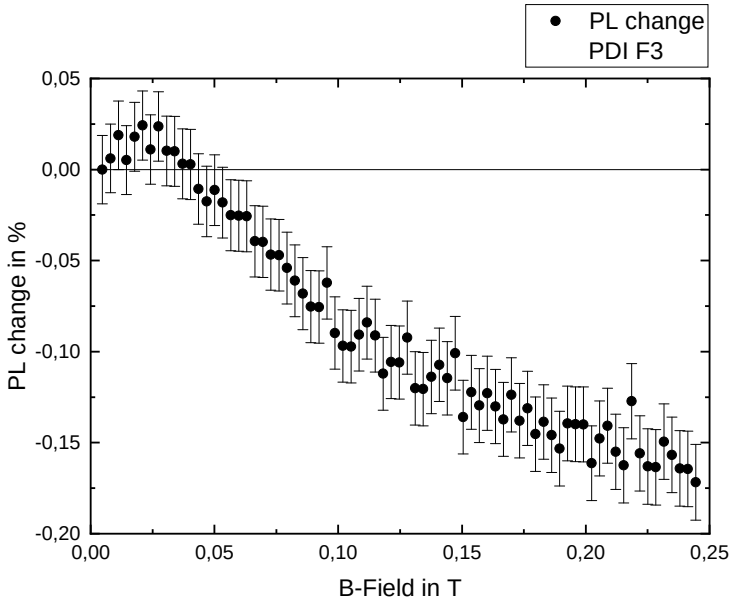

Figure 18: PL change in an external magnetic field of a PDI F3 sample. In contrast to the other PDIs the PL change shows a triplet curve.

This does not meet our expectations for a singlet fission material. But since the triplet curve is clearly visible, the singlet fission process must be involved. It is hard to say why the PL behaves basically in the opposite way compared to the previous samples.
One explanation could be that triplets are radiatively recombining, relaxing into the ground state. This process is referred to as phosphorescence and is a spin-forbidden transition, which is why the radiation intensities are very low compared to the $S_1 - S_0$ transition. Nevertheless, it can occur due to internal or external spin-orbit coupling which mixes pure singlet and triplet states to produce states with a mixed character in spin multiplicity.[12] The phosphorescence intensity is directly correlated to the amount of triplet excitons in the material. This explains why the phosphorescence intensity behaves in shape of the triplet curve if an external magnetic field is applied. But there is no indication why the phosphorescence would outcompete the radiation from the $S_1 - S_0$ transition in this specific molecule. The opposite is the case: A PL spectrum of PDI F3 reveals that the PL peak is at around 700 nm. Assuming this to be the

radiation of the singlets recombining, the triplet energy in a singlet fission material should be roughly half the singlet energy. Meaning that the phosphorescence should happen at wavelengths around 1400 nm. The spectrometer we used in this case did not count photons in a region of wavelengths that high. That is why we can not exclude a large phosphorescence peak there. But the photodetector which was used to measure the PL resulting in the triplet curve in figure 18 was a silicon photodiode. It is not possible that light with wavelengths of 1400 nm is detected with such a device.
If we instead assume that the 700 nm peak is caused by phosphorescence this should mean that the PL of the singlet recombination happens at wavelengths around 350 nm (since $E(S_1) \approx 2E(T_1)$). But this is also not a possible explanation because the laser we used in this experiment has an excitation wavelength of 520 nm. This excitation energy can not excite a singlets whose energy corresponds to a 350 nm emission. When no singlets are excited we would not see a PL signal. Even if there was an excitation of the triplets out of the ground state, which is also spin-forbidden, we would not expect a SF related effect like the triplet curve. The magnetic field effects (chapter 1.3.3) are explained with the assumption of starting with a singlet excitation. For example: A strong B-field is hindering the interconversion between the spin sublevels. Having less triplets in strong fields is therefore a result of less singlets being converted into triplets. If the model started instead with an assumed triplet excitation (which is not very likely anyway), strong fields would result in more triplets because the interconversion is hindered.
The fact that the result is the opposite of the expectation could mean that the ratios of the rate constants k_x of equation (1) are inverted so in this sample the TTA efficiency is stronger than the SF efficiency. This would result in the magnetic field effects basically being turned around. But this is also not a plausible explanation because like written in chapter 1.3.3 the reasons for the MFEs are on the one hand the enhanced interconversion of the spin sublevels in the correlated triplet pair in low fields, and on the other hand the Zeeman splitting in strong fields. These effects, caused by a magnetic field, can not happen in reverse.

There is no reasonable explanation yet for the PDI F3 sample showing a triplet curve. In contrast to the other PDI molecules the PL signal must be coupled to the amount of triplets instead of the singlet amount in the material.

2.3 Tetracene - Low Bandgap Semiconductor Bilayers

In this section the goal is to examine whether excited triplet states, generated from singlet fission, will transfer from the singlet fission material tetracene into a low bandgap semiconductor (either low bandgap perovskite (PRV) or silicon). Therefore the experiment from chapter 2.1 is used again investigating the magnetic field effects and involving PL changes of a bilayer (tetracene–PRV or tetracene–silicon).

2.3.1 Tetracene only

At first we will have a look on the magnetic field effects of tetracene itself without the semiconductor, and clarify how the PL intensity changes during the increase of the magnetic field. A spectrum of the PL of tetracene after excitation with a 405 nm laser is shown in figure 19.

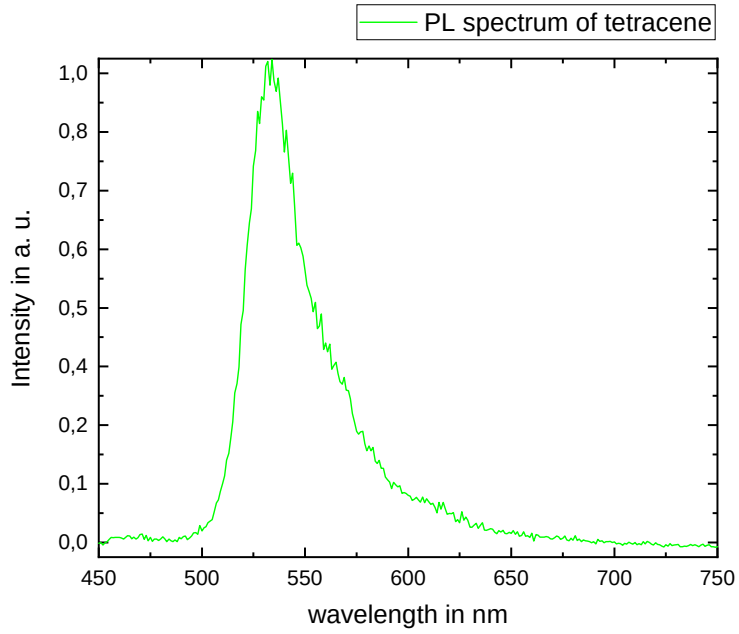

Figure 19: PL Spectrum of tetracene. A sample of tetracene on glass was illuminated by a 405 nm laser diode. There is a PL peak between 530 and 540 nm.

Just like we saw in the PDI measurements, the PL of the tetracene samples (tetracene evaporated on a glass substrate) also becomes lower when they are continuously excited by the laser. But the effect is not that strong compared to the PDI molecules from chapter 2.2. In addition the absolute PL intensity of tetracene is much higher. That is why we still get clear results when we reduce the laser power. This is preventing the degradation of the sample even more. Also the changes of the PL caused by the magnetic field are more significant so the degradation doesn't play such a big role as in chapter 2.2. Even though the PL intensity decrease is still noticeable in the results, as we see in figure 20. So we will also use the stepwise measurement, introduced in figure 13, for the calculation of the PL intensity change.

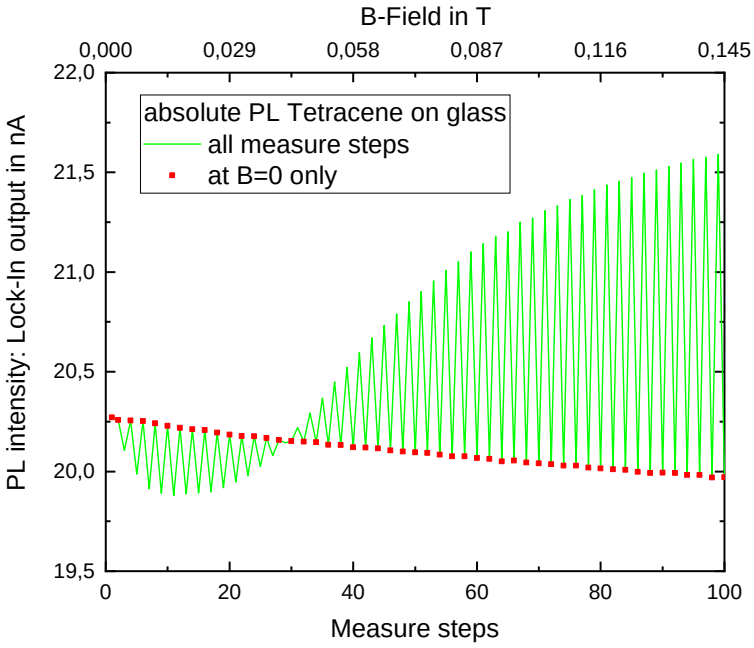

Figure 20: PL change in an external magnetic field of a Tetracene sample. Measurement steps as described in fig. 13.

In figure 20 it is clearly visible by the red dotted line that the intensity loss caused by the degradation involved is not as big as the PL changes caused by the magnet. By seeing the red $I(0)$-line so well, you can already guess from the absolute data that the relative PL change will first turn negative with a minimum at about $B = 0.02\,T$. Then it increases again, changes the sign, and will end up positive. These expectations are confirmed by figure 21.

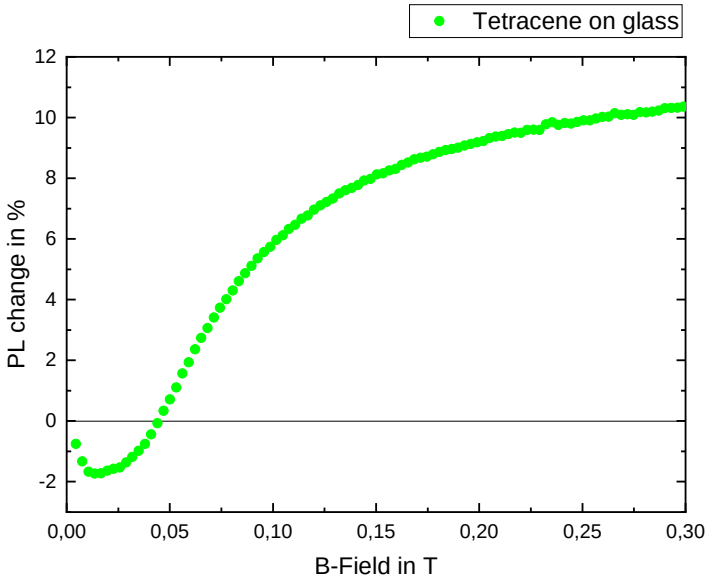

Figure 21: Relative PL change in an external magnetic field of Tetracene.

The PL changes of tetracene, seen in figure 21, show a clear indication of the singlet fission effect since

the curve is almost exactly shaped as in figure 4. It shows the singlet curve because singlet excitons are radiatively recombining, causing the photoluminescence, while triplet excitons are not.
In numbers we see that the PL intensity decreases up to 2% at small B-fields around 0.02 T. The sign change from minus to plus happens at 0.05 T. At 0.3 T the saturation is not completely reached yet but the PL intensity is already more than 10% higher compared to it at B = 0.

2.3.2 Methods

In the following part of the experiment we investigate bilayers of tetracene on top of low bandgap perovskite. In the first measurements with the photodiode we use a perovskite provided by the company `Oxford PV`. The bandgap is assumed to be $E_g = 1.2\,\text{eV}$. Both tin and lead are used as metal cation. But the exact structure is unknown by us since `Oxford PV` is a commercial company that is competing with other companies on the market. On top of the PRV we evaporated a film of tetracene, which was provided by `Sigma Aldrich` with a nominally purity of 99.98%. The thermal evaporator we used is the model `Åmod` by `Ångstrom engineering`. The evaporation speed was $1\,\frac{\text{Å}}{\text{s}}$ and the final thickness of the film is nominally 300 nm.
For another type of sample we deposit a thin film of Al_2O_3 (20 nm) on the perovskite using atomic layer deposition (ALD). After that also 300 nm of tetracene are thermally evaporated on top. Since Al_2O_3 is an isolator the thin interlayer is meant to block a possible exciton transfer between Tc and PRV, but photons can still pass the thin interlayer of 20 nm.

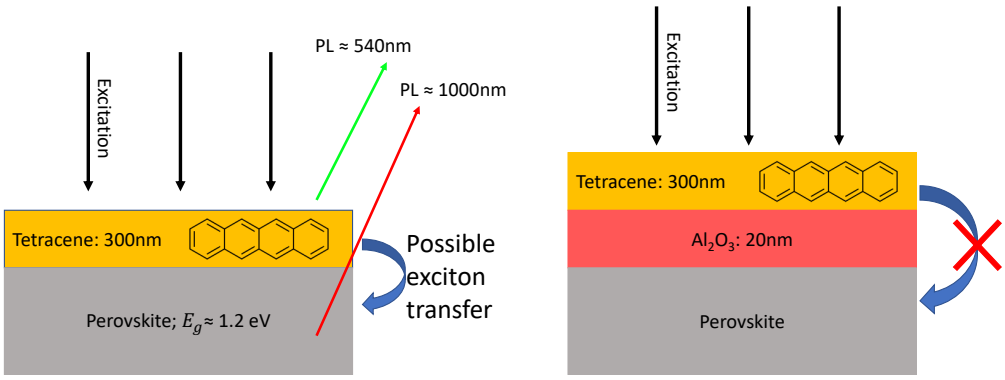

Figure 22: Sample structure: a 300 nm film of tetracene is evaporated on top of low bandgap perovskite (left). A 20 nm Al_2O_3 interlayer between Tc and PRV prevents a direct exciton transfer (right). The PL peak of tetracene appears at about 540 nm (see fig. 19) while the PL of the PRV is expected at about 1000 nm.

In the further execution of the experiment (from the point on when we used the InGaAs spectrometer) we used a different kind of perovskite. Again for the metal cation tin and lead are used while also the organic cation is not uniform but either methylammonium (MA) or formamidinium (FA), so the elemental formula is $(FASnI_3)_{0,6}(MAPbI_3)_{0,4}$. The samples were fabricated following the publication of J. Tong *et al.*[24]. The bandgap is $E_g = 1.25\,\text{eV}$. After the fabrication we again thermally evaporated tetracene on top (100 nm).
Analyzing the PL measurements with the InGaAs spectrometer we found that the intensity of the latter perovskite is way higher than the one of the `Oxford PV` perovskite. A reason could be that the samples are instable and degrade over time. (The `Oxford PV` samples were delivered in March, while our 'own' samples were fabricated in August when the spectrometer experiment was also executed.) This is why

we did the later parts of the experiment with the $(FASnI_3)_{0,6}(MAPbI_3)_{0,4}$. At the moment we do not have a sample of Tc on $(FASnI_3)_{0,6}(MAPbI_3)_{0,4}$ with an Al_2O_3 interlayer yet.

In another attempt we do the same experiments with a tetracene–silicon bilayer. One half of the wafers is n-doped while the other half is undoped. The bare wafers are cut into squares with a side length of 1 cm. After cutting they are put into an HF solution to clean them from contamination and oxidation. Then also a tetracene layer of 100 nm thickness is added on top by thermal evaporation. In the end they are also stored in a nitrogen atmosphere. Bare Silicon has a bandgap energy of $E_g = 1.12\,eV$[9].

2.3.3 Tetracene – low Bandgap Perovskite Bilayers

If we do the same experiment like in chapter 2.3.1 with the tetracene–low bandgap perovskite bilayer, we want to find out whether triplet excitons transfer from the tetracene into the PRV. In the results above with tetracene only, we saw that from the PL of tetracene we can only draw conclusions about the singlet behavior in a magnetic field but not directly about the triplets involved. Even though we expect way more excited triplet states in the tetracene than excited singlets since we assume the singlet fission rate to be very efficient. So if there was an exciton transfer from the tetracene into the PRV we assume way more triplets than singlets to transfer. Also only this would increase the efficiency of a solar cell device. With only singlets transferring into the perovskite the efficiency could not increase because the thermalization losses would still occur since the excited singlets in tetracene have a way higher energy than the bandgap of the perovskite.
What we hope to see in the bilayer experiment is triplet states, generated from singlet fission, transferring to the PRV and radiatively recombine there. So what we're interested in is the PL of the PRV instead of the tetracene PL. Therefore we use an 850 nm longpass filter not only to block the laser reflection but also to block the PL of tetracene which is emitting at smaller wavelengths (see fig. 19).
A repeat of the experiment from above with a bilayer (tetracene–PRV) and an 850 nm longpass filter gives the result shown in figure 23.

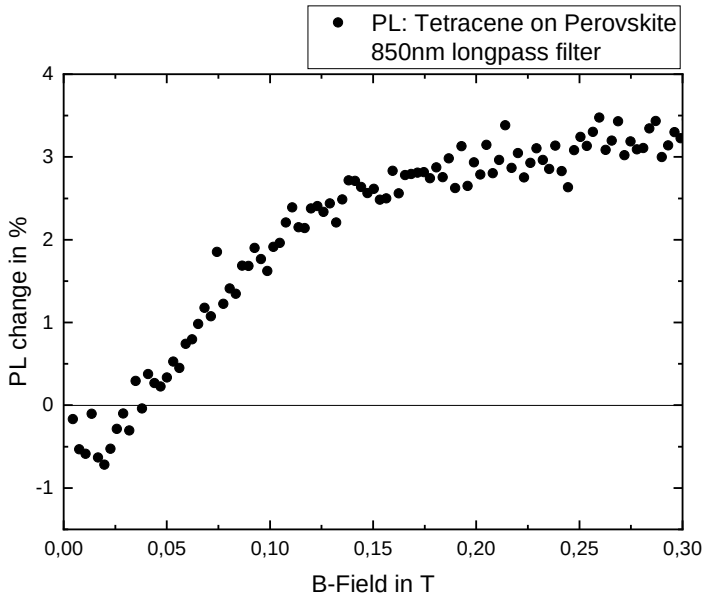

Figure 23: Relative PL change of a tetracene-PRV bilayer above 850 nm.

The PL change is again shaped like a singlet curve. Even if the amount of change in numbers is smaller than seen in the result with tetracene only (fig. 21). But these numbers are not good to compare because the samples were fabricated on different dates and might have some small differences because of different handling and storage.
Anyway, the singlet curve in figure 23 is clearly visible which can have different reasons. If there was both

singlet and triplet transfer into the PRV we would expect the curve being flipped upside down at the zero line. Because the amount of excited triplets in the organic layer is assumed much higher than the amount of excited singlets, we would expect a triplet curve. The radiative recombination processes in the PRV are expected to come from the many transferred triplets instead of the far fewer singlets. The result from figure 23 could indicate that singlet transfer is preferred rather than triplet transfer. One reason for that can be that the energy levels of the two materials do not match well enough. The triplet energy of tetracene is $E(T_1) = 1.25\,\text{eV}$. This should be more or equal to the bandgap energy of the perovskite so triplets of tetracene can excite electrons in the PRV. If the bandgap of the PRV is higher than $E(T_1)$, there is not enough energy to create an electron hole pair in the PRV and a transfer is not possible. The bandgap of the perovskite, provided by our collaborators from `Oxford PV`, is expected to be $E_g = 1.2\,\text{eV}$ and so should match well to $E(T_1)$. However, the singlet exciton energy in tetracene is $E(S_1) = 2.32\,\text{eV}$. This is way higher than the bandgap of the PRV and so Singlet excitons can surely be transferred. If E_g would slightly differ from the expected 1.2 eV, being greater than that, the triplet transfer would be prevented. But singlet transfer is still possible. So this could explain the singlet curve in figure 23.
In order to check if the result comes indeed from a dominant singlet transfer, we repeated the experiment with another sample where we also have tetracene on PRV but with a thin film Al_2O_3 interlayer (thickness: 20 nm) between Tc and PRV (see fig. 22). The film was made by atomic layer deposition (ALD) on the PRV and the tetracene was evaporated on top afterwards (300 nm). By using the Al_2O_3 interlayer we make sure that there is no direct transfer of excitons (neither singlets nor triplets). Excitons cannot pass the isolating interlayer and so not reach the perovskite leading to a PL above 850 nm. So in this case we should see no magnetic field effects on the PL at all since the perovskite PL itself is not effected by a B-field.

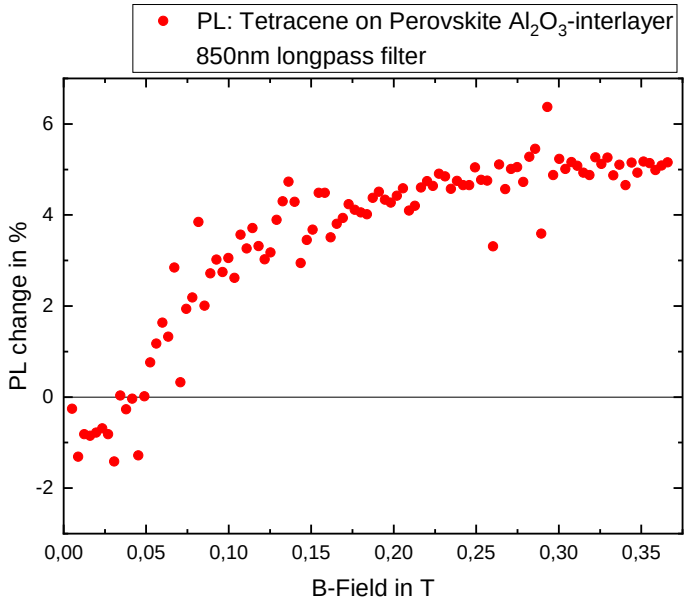

Figure 24: Relative PL change of a tetracene-Al_2O_3-PRV sample at wavelengths above 850 nm. Even with the interlayer which prevents an exciton transfer, the singlet curve is still clearly visible.

But in figure 24 we still see the shape of a singlet curve. With consideration of the filter use, the PL signal seen in this experiment must have a wavelength above 850 nm and so comes most likely from the low bandgap perovskite. Even though the interlayer prevents a transfer of excitons.
So the resulting singlet curve from the experiment without an interlayer (fig. 23) is most likely not explained by singlet exciton transfer from the tetracene to the perovskite.
An explanation for both results with and without an interlayer seeming to be similar can be not only an exciton transfer but a photon transfer instead: By illuminating the sample with the laser, singlet excitons are excited. What we saw in the experiment above with tetracene only, is the photoluminescence (fig. 21). The PL there does only come from excited singlet excitons in the tetracene which recombine

radiatively sending out a photon what we measured in the end. (Triplet excitons can not relax into their ground state since this would be a spin forbidden transition.) These photons appearing from radiative recombination emitted out in any direction. Not only in the direction of our photodetector but also in the direction towards the rear of the sample. In the bi- and trilayer experiments photons could have been emitted by the tetracene and then be reabsorbed again in the perovskite. This can also happen in the sample with the Al_2O_3 interlayer since photons can pass this thin layer. After being absorbed in the PRV, excited electron-hole pairs will lose the excess energy what is above the relatively low bandgap via thermalization. And if they recombine radiatively again they will send out low energy photons which will pass the longpass filter. So the singlet curve we see in figures 23 and 24 could be sort of an echo effect of the singlet behavior in tetracene which we saw in figure 21.

In the next step we will check the theory of the photons being reabsorbed in the perovskite layer after being emitted from the tetracene. This happens indirectly by the use of a spectrometer. We will have a closer look on the PL spectrum of tetracene to figure out if it is really photon transfer through the Al_2O_3 interlayer or if there can be found some other explanation for the singlet curve in figure 24.

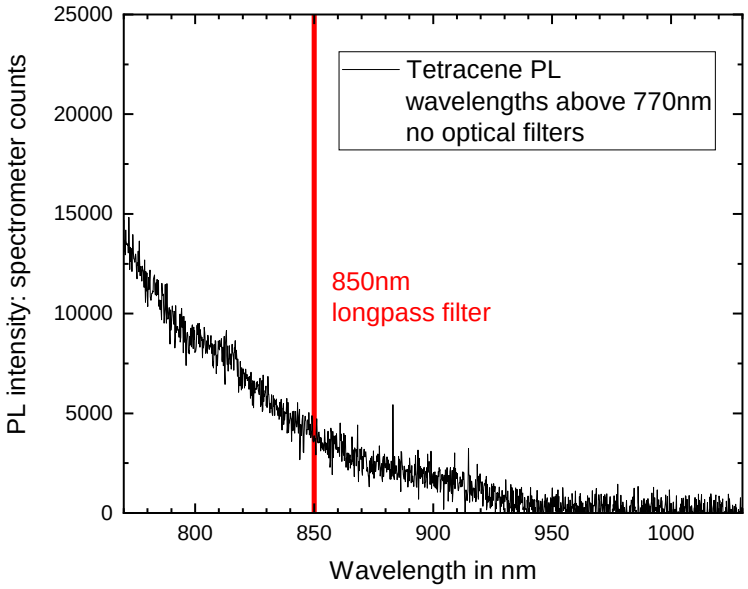

Figure 25: PL spectrum of tetracene at wavelengths above 770 nm. Even at wavelengths above 850 nm the spectrometer can measure a certain intensity.

Considering the tetracene PL spectrum in figure 25 we can see that the spectrometer is still counting a noticeable amount of photons with wavelengths above 850 nm. This means that using the longpass filter in the magnetic field experiments with the bi- and trilayer does not guarantee a complete blocking of the tetracene PL. According to the publication of S. Reineke, M. Baldo *et al.*[18] the appearance of tetracene PL at wavelengths around 900 nm is explained by phosphorescence, an effect occurring through spin-orbit coupling which makes it possible that also triplet excitons can relax into the ground state emitting a photon. But since we still measure a singlet curve at wavelengths above 850 nm it can rather be explained by the singlet emission being very broad in our case.
So it cannot be determined with certainty whether the singlet curves in the figures 23 and 24 come from a photon transfer and reabsorption in the PRV or from the appearance of the tetracene PL above 850 nm.

To distinguish whether the PL signal comes from the Tc or PRV layer in our following results, we will use an InGaAs spectrometer. It is suitable for larger wavelengths so we can focus on the PL of the perovskite layer.

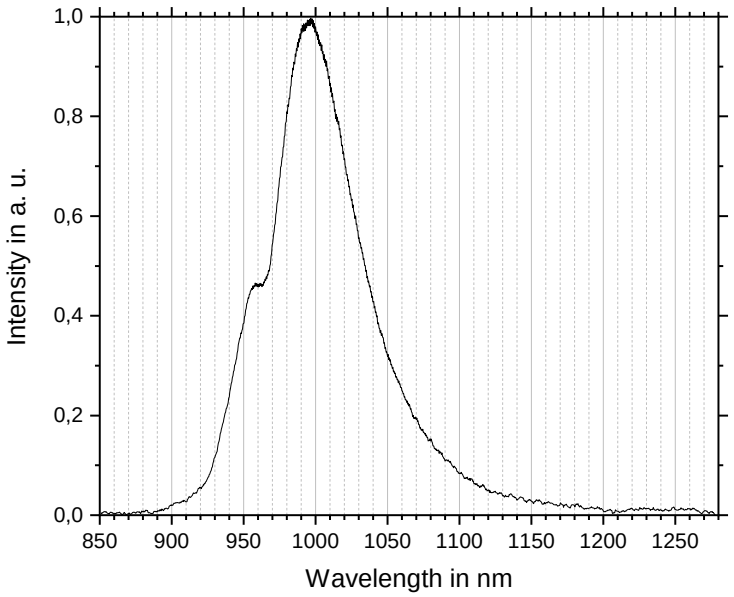

Figure 26: PL spectrum of the low bandgap perovskite, measured with the InGaAs spectrometer. There is a peak at 1000 nm and a shoulder at 960 nm.

Considering figure 26 and as we know at which wavelengths the PL of the PRV occurs, we should be able to observe whether the use of a magnet has an influence on it. If the intensity of the PL at 1000 nm changes significantly by increasing an external magnetic field then there must be a transfer of excitons from the Tc to the PRV. The experiment is now repeated, not measuring with the InGaAs photodiode but with the InGaAs spectrometer. The advantage of the spectrometer is that we can clearly see at which wavelengths changes in the intensity appear. But a big disadvantage is that it is using a software which is not synchronized with the magnet. So every time we increase the magnetic field, we have to give the command of acquiring a spectrum by hand (this was happening automatically using the photodiode). It is a disadvantage in the sense that the times of illumination of the sample will not be the exact same at each measuring step. For example: If the spectrum is measured at a certain magnetic field $B = x$, then the increasing of the B-field to $B = y$ takes the operating person two seconds. A new spectrum is acquired and the increasing to the next step $B = z$ would take the person three seconds before the next measurement. Now the illumination times between the two steps are different. This will matter if the PRV degrades in a similar way like the tetracene and PDIs did in the results above, when being constantly illuminated by the laser. Taking that into account, we will only focus on the possible differences of the spectra between $B = 0\,T$ and $B = 0.3\,T$. According to the PL changes of tetracene, seen in figure 21, we assume the changes in PL to be more significant and to have a higher chance to see changes at all. At small changes in small magnetic fields we cannot guarantee a measurement precise enough to see those (because of the disadvantage described above).

If there are changes in the PL intensity in different measurements we have to distinguish whether it is an appearance caused by the magnet or by the degradation. So what we do in the end to compare spectra with magnet on ($B = 0.3\,T$) and magnet off ($B = 0\,T$) as well as possible, is measuring those spectra with the magnet turned on and off alternately. One series of measurements is shown in figure 27.

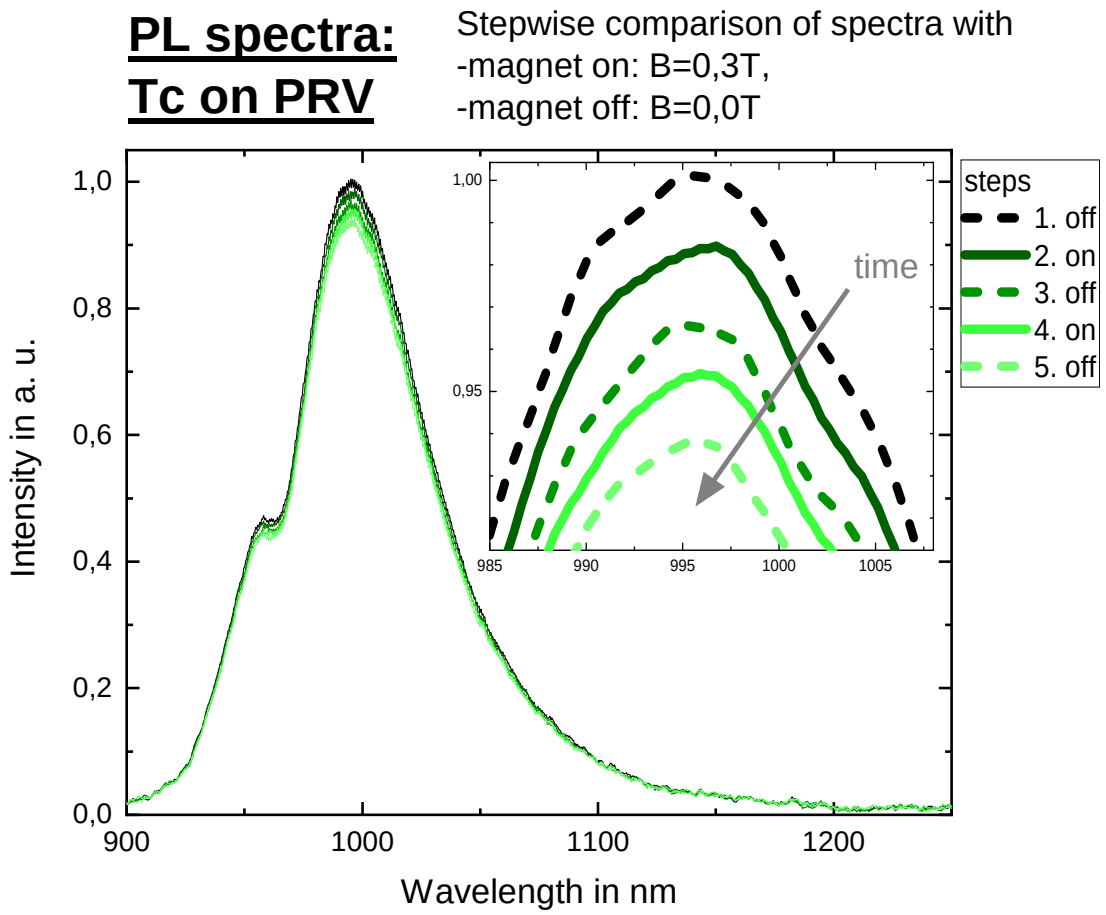

Figure 27: PL spectra of the Tc-PRV bilayer. Comparison of B = 0 T and B = 0.3 T. The spectra have been acquired with alternately magnet off (dotted lines) and magnet on (solid lines). In the peak region it becomes visible, that the intensity decreases after every measurement step.

By the method of the alternate measurements with and without a magnetic field (fig. 27) it is visible that the intensity of the PRV PL is decreasing after every measuring step. It does not seem to play a role whether the magnet is turned on or not. It rather seems like the decrease was only a matter of time. The integration time of the spectrometer was 8 s per spectrum. If there was an exciton transfer from the tetracene to the PRV, the PL change from that must be smaller than the PL decrease caused by degradation.
In figure 27 it is only visible that there is a certain decrease in intensity after every step. But from the spectrum it can not really be said whether the decrease is stronger between magnet off – magnet on or between magnet on – magnet off. To quantify this decrease, all the spectrometer counts collected in the PL peak area between 970 nm and 1030 nm are summed up and plotted step-resolved in figure 28. This is done for every single spectrum. We collected 20 spectra (10 with magnet on, 10 with magnet off alternately). Integrating the counts in the peak area gives 20 data points, each belonging to one spectrum. 'Step-resolved' can be replaced by time-resolved when it is assumed that the operating person measured the different spectra in a constant rhythm. Such that the illumination time is the same between two consecutive spectra.

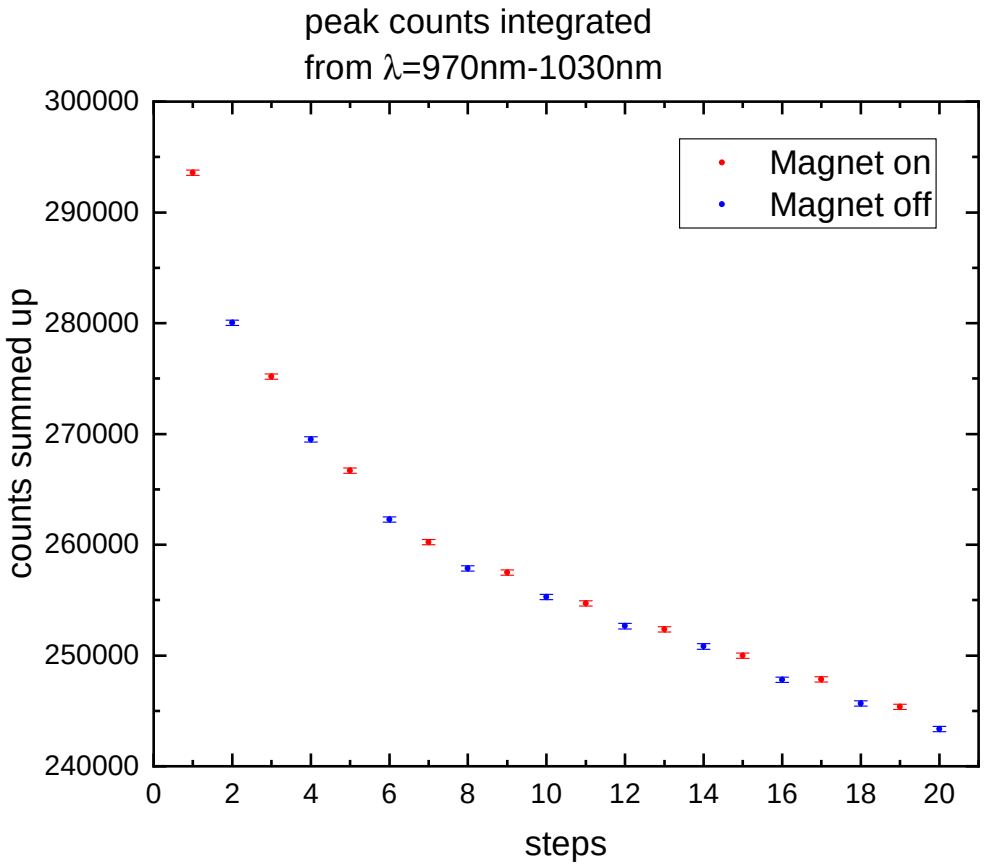

Figure 28: All the spectrometer counts in the peak area of 970 nm–1030 nm are summed up. This is done respectively at every measuring step so every data point represents one spectrum. The spectra were measured alternately with a magnetic field of B = 0.3 T (red) and B = 0 T (blue).

In figure 28 it is again clearly visible that the PL intensity decreases the longer the sample is illuminated. At the beginning of the measurement, a few seconds after the laser is turned on, the degradation is the strongest. After about one minute (from step 6 on) the decrease in intensity seems to end up linear. If the external magnetic field had no effect on the PL signal of the PRV, the blue and red points in figure 28 should lay on one common line. But this is actually not the case. The red points are slightly shifted upwards, which can be seen in the 'linear part' of figure 28. In figure 29 this becomes clearer. A linear function is added through the red points (magnet on), calculated with the data in the area from step seven on. The same is done with the blue data points (magnet off) from step eight on. Both of the functions (red and blue) have a similar slope, but are slightly shifted. The red one is shifted upwards 1140(450) counts.

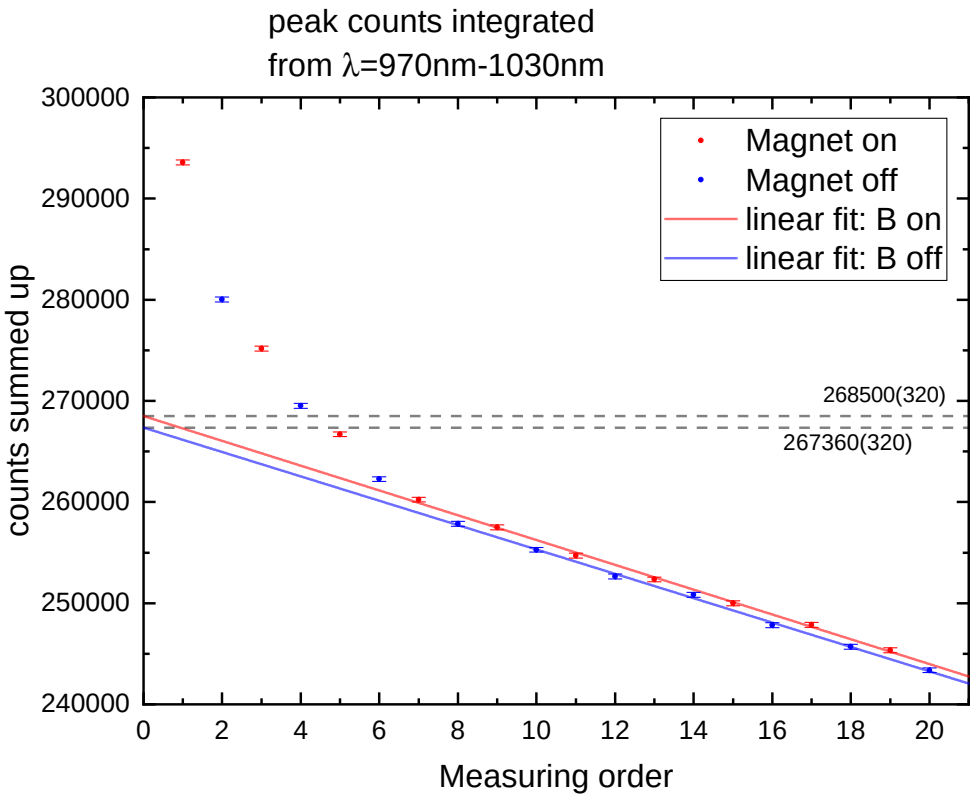

Figure 29: All the spectrometer counts in the peak area of 970 nm–1030 nm are summed up. This is done respectively at every measuring step so every data point represents one spectrum. The spectra were measured alternately with a magnetic field of B = 0.3 T (red) and B = 0 T (blue). Fitting a linear function to both the data (magnet on/off) respectively shows that the PL intensity with an external magnetic field is slightly higher. At the y-intercept the red curve is shifted 1140(450) counts upwards.

The fact that the red curve (magnet on) in figure 29 is shifted upwards compared to the blue one (magnet off) indicates, that the PL intensity of the PRV is higher when a B-field is applied. Because we focused on the peak region, it can be ruled out that the PL change is a direct appearance of the tetracene layer. So it is sure that it is a change in the PRV PL. As we compare the shift of 1140(450) counts to the y-axis intercept of the blue (magnet off) line we can calculate a relative PL change similar to the calculation (2) above.

$$\text{PL change}(\text{B} = 0.3\,\text{T}) = \frac{268\,500(320) - 267\,360(320)}{267\,360(320)} = \frac{1140(450)}{267\,360(320)} = 0.0043(17) \tag{3}$$

So the PL change of the low bandgap perovskite under the Tc layer increases 0.43(17)% if a magnetic field of B = 0.3 T is applied. As we see in the PL change of tetracene itself in a B-field (fig. 21), it was confirmed what is predicted in chapter 1.3.3: In an external B-field the amount of singlets in the tetracene increases at fields around B = 0.3 T, compared to B = 0 T. The amount of triplets instead decreases. So what we can conclude from the result of figure 29 is that the increasing of the PRV PL must be connected to the amount of singlets in the tetracene.
Again there are the two explanations already mentioned above: 1) the photon transfer and reabsorption of the Tc PL in the PRV or 2) the singlet transfer being preferred rather than triplet transfer. In this part of the experiment with the InGaAs spectrometer we do not have a sample of Tc on PRV with an Al_2O_3 interlayer. So we cannot make sure which reason is mainly leading to the PL increase in the B-field.
As mentioned in chapter 2.3.2 the bandgap of the PRV we used in this part is supposed to be $E_g = 1.25$ eV

which is exactly matching with the triplet energy $E(T_1)$ of tetracene. The PL peak of the PRV which we see in figure 26 is at 997 nm which corresponds to an energy of 1.244 eV. If we assume the PL energy to be equal to the bandgap energy, E_g is even slightly below $E(T_1)$ of Tc. So this should not be ruling out a triplet transfer. Furthermore it is not explained by that, that singlet transfer would be preferred.
If we instead assume a STOKES shift at the PL of the PRV, the bandgap energy would be higher then the energy of the photons emitted again. Because the energy levels of the PRV and the triplet state in tetracene are so close to each other it could be possible that the bandgap is actually higher than 1.25 eV. This would prevent a triplet transfer. If that was the case, only singlet transfer would happen and explain why the PRV PL becomes stronger in a high B-field. In order to rule out the exciton transfer to explain the PL increase, the measurement should be repeated with the Al_2O_3 interlayer.
On the other hand, the effect coming from a photon transfer is also likely. Since the PL of tetracene is clearly visible for the operating person, photons emitted by a radiative singlet relaxation could as well be absorbed by the PRV. And since these reemitted photons become more in a B-field of 0.3 T (fig. 21) the absorption in the PRV is increased as well.
In the latter case it could well be that no actual exciton transfer takes place at all. One explanation for that is that the DEXTER energy transfer, explained in chapter 1.3.2 is not favorable at the interface between tetracene and perovskite. In order of DET to happen, there must be a proper wave function overlap between the donor (Tc molecule) and the acceptor (PRV). It could be that the alignment of the tetracene molecules at the interface is not favourable for that. For the spatial wave function area it is essential whether the molecules are standing on the interface like pillars or if they lie on the interface. The molecular alignment of the tetracene at the interface is not well known yet.

However, the fact that the PRV PL is increased by a singlet related effect indicates, that the efficiency of a potential solar cell device would not be increased. The original idea was that high energy photons with an energy above $E(S_1) = 2.32$ eV would be absorbed in the tetracene. Through the singlet fission process, two triplet excitons are created. If they transferred into the semiconductor creating e-h-pairs, the quantum efficiency for these high energy photons would have been doubled. If instead singlets are transferred (either via an exciton transfer or via a photon) it doesn't make a difference in efficiency combined to a perovskite cell without tetracene. The energy excess of the photons is still lost via thermalization.

2.3.4 Tetracene–Silicon Bilayers

The last part of the experiment mentioned above (the use of the InGaAs spectrometer in combination with the magnet) is repeated with the tetracene–silicon bilayers. Either n-doped as well as undoped silicon is used with a tetracene layer on top.
At first we will again have a look on the PL spectrum of a bare silicon wafer with the InGaAs spectrometer.

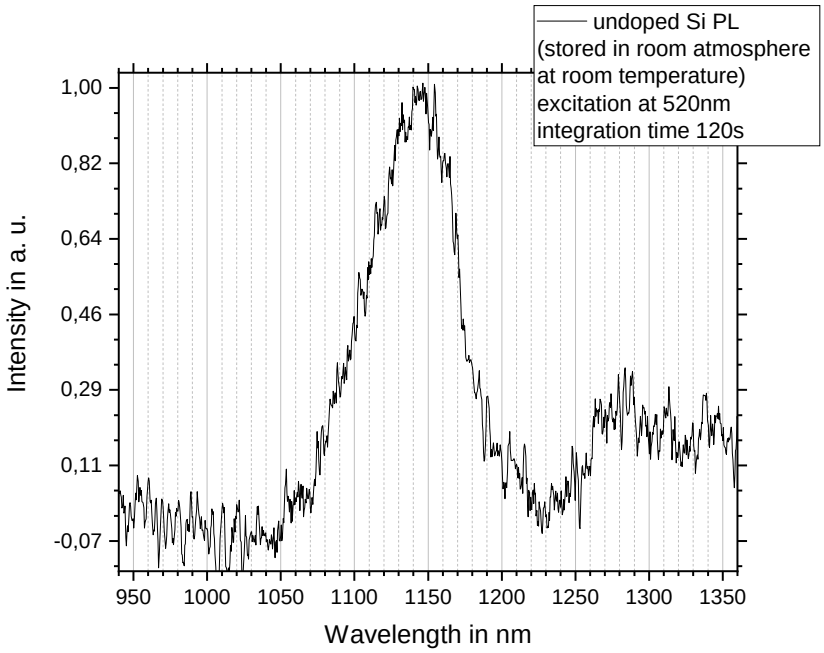

Figure 30: PL spectrum of an undoped silicon wafer which was stored under normal atmosphere conditions without special treatment. A peak is visible at 1150 nm and another appearance from 1270 nm on.

As we see in figure 30 the PL spectrum of silicon is much noisier than for example the spectrum of the PRV in figure 26. Even though the measuring time here of 120 s is much longer than in the PRV measurements (8 s), the amount of photons detected in the silicon spectrum is more than one order of magnitude lower. This is explaining why the spectrum in figure 30 does not look that smooth because the signal to noise ratio is much smaller. Even though we managed to measure a peak at 1150 nm with a weak shoulder at 1200 nm which has been similarly measured by other groups before.[4] But also we see a signal from 1270 nm on which can not be explained for now. The noise level in this measurement is so high that it is hard to say whether it is a real effect of the silicon or not. The same argument applies for the 'shoulder' at 1200 nm. Also it could be that the experiment was not covered well enough from incident room light.

The experiment from chapter 2.3.3 is repeated with the Tc–Si bilayers to compare the PL intensities when a magnet is used. The spectra without an applied magnetic field are shown in figures 31 (undoped) and 32 (n-doped).

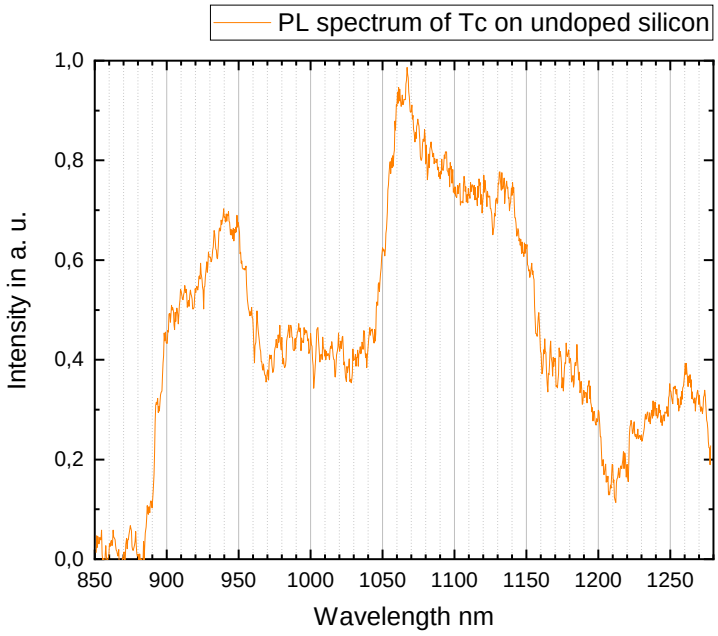

Figure 31: PL spectrum of a Tc–Si bilayer (undoped silicon).

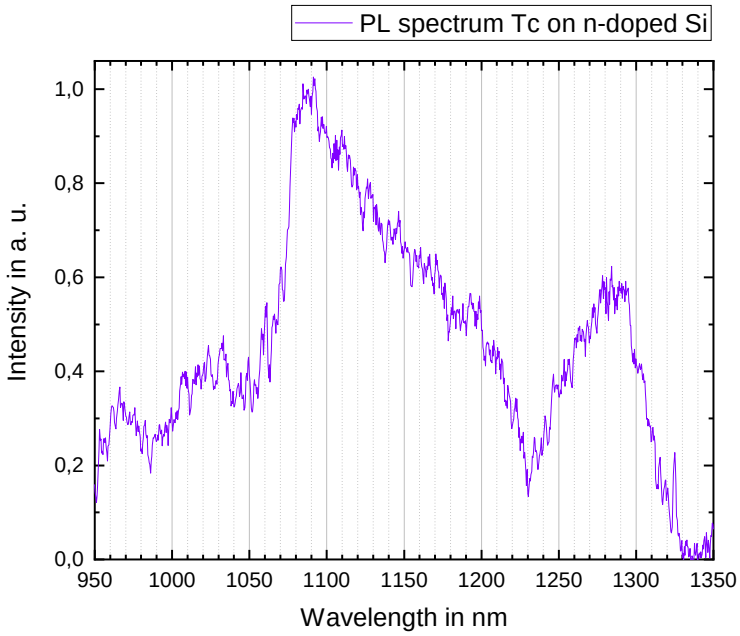

Figure 32: PL spectrum of a Tc–Si bilayer (n-doped silicon).

Comparing both spectra it becomes evident that they look completely different from the one in figure 30 with bare silicon. The highest peak in both cases is rather at 1070 nm than at 1150 nm. Both the spectra 31 and 32 are measured at different wavelength ranges which makes it harder to compare them since we can not compare the PL intensities at wavelengths up to 950 nm and wavelengths from 1250 nm on. Similarities are seen in the highest peak wavelength in both cases and a minimum at roughly 1220 nm. A

clear difference is that in the n-doped case the amount of counts seem to decrease continuously between the maximum and minimum while in the doped case there is a relatively sharp edge at 1150 nm. Also noticeable is that before and after the peak the intensity is not even close to zero but rather in a moderate intensity region. It would be interesting to measure spectra with a broader range of wavelengths to see how the PL intensities develop both left and right hand side of the peak.
It is hard to say why the spectra show these trends. It could be that these are appearances of the PL of the tetracene film which is on top of both the silicon samples. We know that the PL does not reach these high wavelength regions but coincidental the highest intensity in the spectra 31 and 32 are at double wavelength of the tetracene PL peak (compare with fig. 19). So one guess is tetracene emission causing interference effects which appear to cause radiation at double wavelength. But this is very unlikely since then we should also see such an appearance caused by the laser at a wavelength of $1040\,\text{nm} = 2 \cdot 520\,\text{nm}$ which should be really intense according to a high laser power.
An appearance of the silicon PL how it is seen in figure 30 is not visible. In figure 31 the intensity drops down relatively sharp just before 1150 nm and in figure 32 we observe a continuous decrease in intensity at 1150 nm.
Another explanation why the spectra of the silicon substrates with tetracene look so different from the one with bare silicon could be the encapsulation. Unlike in the measurements with the bilayers which were encapsulated to prevent the tetracene and the silicon from contamination, the bare silicon wafer was illuminated without being encapsulated. So this could be the reason why both the bilayers have spectra that look similar to each other but different from the bare wafer. The main difference, apart from the tetracene, is given by the glass plate which protects the samples from contamination. So the spectra we see in figures 31 and 32 could possibly show an effect of glass being illuminated by the laser. The fact that we see no appearance of the Si-PL similar to figure 30 could be explained by the difficulty to measure a silicon PL signal at all. It took many attempts to measure a spectrum like 30. The intensities were very low: Even with an integration time of the spectrometer of two minutes, only less than 300 photon counts were collected at the highest peak area at the best attempt. The position of the illumination spot and the orientation of the silicon plate played a big role. Only if the combination of these circumstances was perfect we could see a signal at all. In all of the other attempts we were not able to collect enough photons with the spectrometer. So it might well be that we simply did not measure a Si-PL in the attempts when we investigated the encapsulated bilayers, but only some effects from the glass.

Again the magnet is used to examine whether the spectra will look different at a magnetic field of $B = 0.3\,\text{T}$. In figure 33 two of these spectra are depicted while a sample of undoped silicon was used.

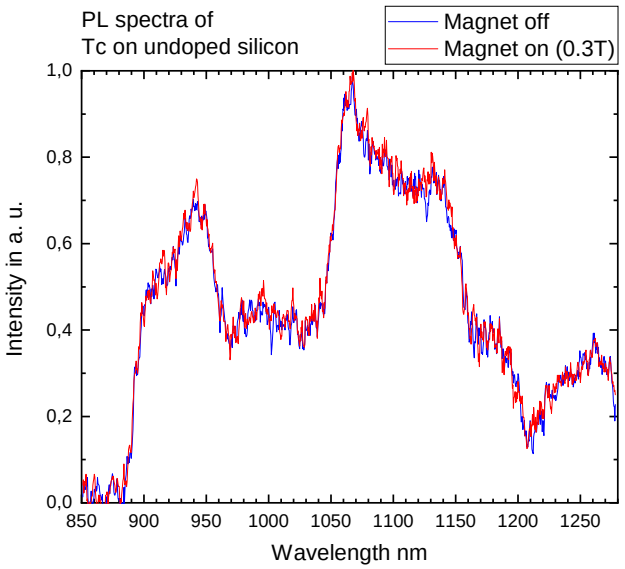

Figure 33: PL spectra of a tetracene–undoped silicon bilayer. Comparison of the spectrum with an external magnetic field of $B = 0.3\,\text{T}$ (red) and without a magnetic field (blue).

In figure 33 there is no clear difference noticeable between the spectra with the magnet turned on (red) an off (blue). The two curves are so noisy that even when there was a slight difference in intensity we could not notice it just from looking at figure 33. Therefore we again use the method of integrating all the spectrometer counts of the whole spectrum and plot them step resolved.

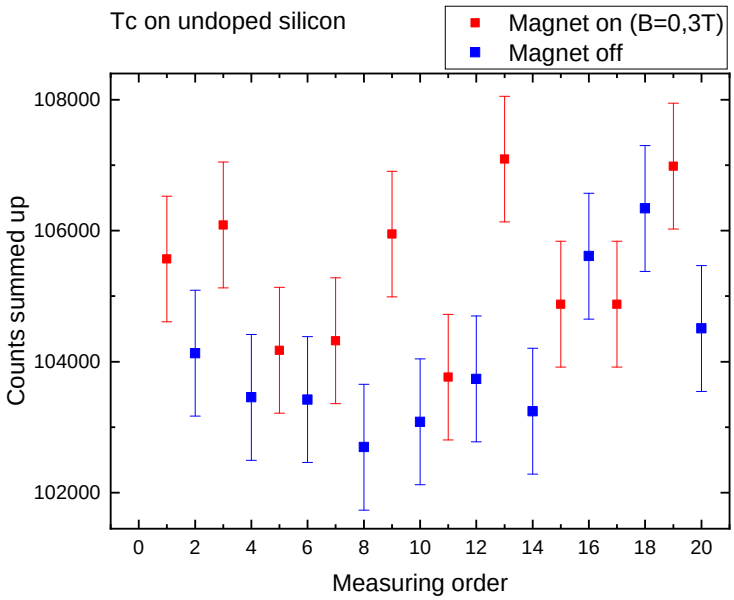

Figure 34: Tetracene on undoped silicon: spectrometer counts of all wavelengths summed up respectively for every measurement (every data point represents one spectrum). Comparison of spectra, measured at B = 0.3 T (red) and at B = 0 (blue). The magnet was turned on and off alternately. Error bars are relatively large because the spectrometer counts of the actual measurement are in the same order of magnitude as from the background spectrum which was subtracted. (In the attempts with the PRV in chapter 2.3.3 the amount of PL counts outnumbers the subtracted background counts by orders of magnitude.)

Figure 34 does not give more information about whether there is a connection between the tetracene singlet fission process and the PL intensity of the silicon. The data points are almost randomly spread and the uncertainties are too big to draw any quantitative conclusions.
When we repeated the measurement one more time with the n-doped silicon we could not manage to get results with enough photons anymore. On account of this, the comparison of spectra with and without an external B-field is missing.

So to conclude, from the data collected above it is not possible to make a statement about whether the tetracene interacts with the silicon wafer or not. As we are not sure whether we see a silicon PL signal in the spectra 31 and 32 or only undesired effects of the glass being illuminated, we can not draw conclusions about the Tc–Si interaction. The method with the magnet does not give any further information in this case.

3 Conclusion & Outlook

It has been confirmed that using the magnetic field effects occurring in singlet fission materials is a good way to detect the singlet fission process. By investigating the PL intensity change in an external magnetic field, new SF materials like PDI F8, F15 and F16 were found. The result of PDI F3 showing a triplet curve is not completely understood yet. Further research about the molecular packing of the PDIs has to be done to achieve a deeper understanding about the rate constants and efficiency of singlet fission. Also more PDI molecules with different functional groups need to be investigated for their PL behavior in a B-field to make reasonable statements about the influence of the functional groups on the singlet fission process.

The experimental results of the tetracene–low bandgap semiconductor bilayer indicate that there is no efficient triplet transfer from the SF material tetracene to the solar cell material. It was found that the PL intensity of the PRV is increased at strong external B-fields which corresponds to a singlet related effect. It can be explained by either singlet transfer between Tc and PRV being preferred rather than triplet transfer or by photon emission from the Tc PL and reabsorption in the PRV. To determine the reason, the experiment must be repeated with an isolating interlayer in order to rule out a singlet exciton transfer.
If it turns out that singlets transfer to the PRV, it might be that the energies of T_1 and the bandgap of PRV do not match well. In this case it can be investigated whether the triplet transfer works better if PRVs with slightly smaller bandgap energies are used.
It could also turn out that the result in chapter 2.3.3 is caused by photon transfer and that an exciton transfer is not happening. In this case the way of transfer of the triplet into the PRV requires a deeper understanding concerning molecular alignment and wave function overlap at the interface.

By investigating the tetracene-silicon bilayer we could not observe any magnetic field effect and so we can not make any statements about a possible exciton energy transfer. The problem, using this method of PL change observation, is the very low PL intensities of silicon. With the tetracene layer on top it is hard to detect any signal which we are sure of that it comes from the silicon. In this case a more reliable method would be to contact the silicon wafer and to measure the photocurrent. Since we expect high SF efficiency, the current should correlate to the triplet amount. When the transfer is efficient, the current signal should therefore follow the triplet curve when an external B-field is applied.

To improve the measurement technique, the magnet can be connected to the InGaAs spectrometer in such a way that a B-field step is synchronized with the measurement of one spectrum. Then the spectra could be applied in a constant rhythm. This would make it possible to better quantify the degradation process of the investigated materials. This is not properly achieved yet by doing the measurement by hand.
Another method to improve the results would be to have a shifting plate which allows to vary the position of the illuminated spot in the sample plane. If the sample was shifted after every measuring point the degradation could be prevented. The shifting plate would be a way better method than doing it by hand. The different placing and angle of the sample largely affects the incoupling of the PL signal. The absolute PL intensities measured by the diode are varying heavily in different attempts of measuring the same sample in another position. In the past, the clamping mechanism had to be removed and clamped again. Also the covering plate which protects the setup from incident light had to be removed and added after every shift of the sample by hand. Too many parameters are varied to make different measurements comparable. This would be enhanced by a plate shifting the sample which is controllable from the distance or runs automatically.

References

[1] M. B. Smith and J. Michl. Singlet Fission. *Chemical Reviews*, 110(11):6891–6936, 11 2010. doi: 10.1021/cr1002613.

[2] D. L. Dexter. A theory of sensitized luminescence in solids. *The Journal of Chemical Physics*, 21 (5):836–850, 1953. ISSN 00219606. doi: 10.1063/1.1699044.

[3] S. W. Eaton, L. E. Shoer, S. D. Karlen, S. M. Dyar, E. A. Margulies, B. S. Veldkamp, C. Ramanan, D. A. Hartzler, S. Savikhin, T. J. Marks, and M. R. Wasielewski. Singlet exciton fission in polycrystalline thin films of a slip-stacked perylenediimide. *Journal of the American Chemical Society*, 135 (39):14701–14712, 2013. ISSN 00027863. doi: 10.1021/ja4053174.

[4] T. Fuyuki, H. Kondo, T. Yamazaki, Y. Takahashi, and Y. Uraoka. Photographic surveying of minority carrier diffusion length in polycrystalline silicon solar cells by electroluminescence. *Applied Physics Letters*, 86(26):1–3, 2005. ISSN 00036951. doi: 10.1063/1.1978979.

[5] M. A. Green. Improved value for the silicon free exciton binding energy. *AIP Advances*, 3(11):0–15, 2013. ISSN 21583226. doi: 10.1063/1.4828730.

[6] M. A. Green, A. Ho-Baillie, and H. J. Snaith. The emergence of perovskite solar cells. *Nature Photonics*, 8:506, 6 2014. URL `https://doi.org/10.1038/nphoton.2014.134http://10.0.4.14/nphoton.2014.134`.

[7] M. A. Green, E. D. Dunlop, D. H. Levi, J. Hohl-Ebinger, M. Yoshita, and A. W. Ho-Baillie. Solar cell efficiency tables (version 54). *Progress in Photovoltaics: Research and Applications*, 27(7):565–575, 2019. ISSN 1099159X. doi: 10.1002/pip.3171.

[8] R. C. Johnson and R. E. Merrifield. Effects of magnetic fields on the mutual annihilation of triplet excitons in anthracene crystals. *Physical Review B*, 1(2):896–902, 1970. ISSN 01631829. doi: 10.1103/PhysRevB.1.896.

[9] S. Kasap and P. Capper. *Springer Handbook of Electronic and Photonic Materials*. Springer International Publishing, Saskatoon, Canada, 2006. ISBN 9783319489339. doi: 10.1007/978-3-319-48933-9.

[10] M. Knupfer. Exciton binding energies in organic semiconductors. *Applied Physics A: Materials Science and Processing*, 77(5):623–626, 2003. ISSN 09478396. doi: 10.1007/s00339-003-2182-9.

[11] A. B. Kolomeisky, X. Feng, and A. I. Krylov. A simple kinetic model for singlet fission: A role of electronic and entropic contributions to macroscopic rates. *Journal of Physical Chemistry C*, 118 (10):5188–5195, 2014. ISSN 19327455. doi: 10.1021/jp4128176.

[12] J. Kuijt, F. Ariese, U. A. Brinkman, and C. Gooijer. Room temperature phosphorescence in the liquid state as a tool in analytical chemistry. *Analytica Chimica Acta*, 488(2):135–171, 2003. ISSN 00032670. doi: 10.1016/S0003-2670(03)00675-5.

[13] S. Luo and W. A. Daoud. Recent progress in organic-inorganic halide perovskite solar cells: Mechanisms and material design. *Journal of Materials Chemistry A*, 3(17):8992–9010, 2015. ISSN 20507496. doi: 10.1039/c4ta04953e.

[14] P. M. Zimmerman, F. Bell, D. Casanova, and M. Head-Gordon. Mechanism for Singlet Fission in Pentacene and Tetracene: From Single Exciton to Two Triplets. *Journal of the American Chemical Society*, 133(49):19944–19952, 11 2011. doi: 10.1021/ja208431r.

[15] A. Miyata, A. Mitioglu, P. Plochocka, O. Portugall, J. T. W. Wang, S. D. Stranks, H. J. Snaith, and R. J. Nicholas. Direct measurement of the exciton binding energy and effective masses for charge carriers in organic-inorganic tri-halide perovskites. *Nature Physics*, 11(7):582–587, 2015. ISSN 17452481. doi: 10.1038/nphys3357.

[16] C. T. P. T. Nathalie Girouard, Elianna Konialis. OECDgreen growth. *OECD Green Growth Studies: Energie*, page 106, 2011.

[17] NREL. Best Research-Cell Efficiency Chart, 2019. URL `https://www.nrel.gov/pv/cell-efficiency.html`.

[18] S. Reineke and M. A. Baldo. Room temperature triplet state spectroscopy of organic semiconductors. *Scientific Reports*, 4:1–8, 2014. ISSN 20452322. doi: 10.1038/srep03797.

[19] S. Rühle. Tabulated values of the Shockley-Queisser limit for single junction solar cells. *Solar Energy*, 130:139–147, 2016. ISSN 0038092X. doi: 10.1016/j.solener.2016.02.015.

[20] O. Semonin, J. M. Luther, and M. C. Beard. Multiple exciton generation in a quantum dot solar cell, 2012.

[21] W. Shockley and H. J. Queisser. Detailed balance limit of efficiency of p-n junction solar cells. *Journal of Applied Physics*, 32(3):510–519, 1961. ISSN 00218979. doi: 10.1063/1.1736034.

[22] Tetracene. Wikipedia, 2019. URL `https://en.wikipedia.org/wiki/Tetracene`.

[23] Y. Tomkiewicz, R. P. Groff, and P. Avakian. Spectroscopic approach to energetics of exciton fission and fusion in tetracene crystals. *The Journal of Chemical Physics*, 54(10):4504–4507, 1971. ISSN 00219606. doi: 10.1063/1.1674702.

[24] J. Tong, Z. Song, D. H. Kim, X. Chen, C. Chen, A. F. Palmstrom, P. F. Ndione, M. O. Reese, S. P. Dunfield, O. G. Reid, J. Liu, F. Zhang, S. P. Harvey, Z. Li, S. T. Christensen, G. Teeter, D. Zhao, M. M. Al-Jassim, M. F. Van Hest, M. C. Beard, S. E. Shaheen, J. J. Berry, Y. Yan, and K. Zhu. Carrier lifetimes of >1 ms in Sn-Pb perovskites enable efficient all-perovskite tandem solar cells. *Science*, 364(6439):475–479, 2019. ISSN 10959203. doi: 10.1126/science.aav7911.

[25] G. Vaubel and H. Kallmann. Diffusion Length and Lifetime of Triplet Excitons and Crystal Absorption Coefficient in Tetracene Determined from Photocurrent Measurements. *Physica Status Solidi (B)*, 35(2):789–792, 1969. ISSN 15213951. doi: 10.1002/pssb.19690350228.

[26] M. Wakasa, T. Yago, Y. Sonoda, and R. Katoh. Structure and dynamics of triplet-exciton pairs generated from singlet fission studied via magnetic field effects. *Communications Chemistry*, 1(1): 1–6, 2018. ISSN 2399-3669. doi: 10.1038/s42004-018-0008-0. URL `http://dx.doi.org/10.1038/s42004-018-0008-0`.

[27] X. Wang, R. R. Valiev, T. Y. Ohulchanskyy, H. Ågren, C. Yang, and G. Chen. Dye-sensitized lanthanide-doped upconversion nanoparticles. *Chemical Society Reviews*, 46(14):4150–4167, 2017. ISSN 14604744. doi: 10.1039/c7cs00053g.

[28] K. Yoshikawa, H. Kawasaki, W. Yoshida, T. Irie, K. Konishi, K. Nakano, T. Uto, D. Adachi, M. Kanematsu, H. Uzu, and K. Yamamoto. Silicon heterojunction solar cell with interdigitated back contacts for a photoconversion efficiency over 26%. *Nature Energy*, 2(5):17032, 2017. ISSN 2058-7546. doi: 10.1038/nenergy.2017.32. URL `https://doi.org/10.1038/nenergy.2017.32`.

List of Figures

Acknowledgments

First and foremost I'd like to thank my supervisor **Benjamin**. Not only for showing me what to do, teaching me what I needed to know and always being available for major and minor questions. But also for involving me into the matter so much that I didn't ever have the feeling of being supervised but rather of being part of a good team.
Thank you **Bruno** for giving me the opportunity to come to the Hybrid Solar Cells group to work with you and to write this thesis. Thank you for inviting me to AMOLF.
Thanks to **Silvia** for the fabrication of those excellent low bandgap perovskites, but even more for some nice, productive and fun time we spent together in the lab.
Also thanks to my former colleague **Joris** who supported me during my first weeks and for not hesitating to quickly buy a pen to explain science to me.
Special thanks to the whole **Hybrid Solar Cells group**. You were so welcoming from the first moment on I arrived. The atmosphere in the group was always nice and happy. I really appreciate having worked with all of you and that I have met you all.
I would like to thank **Kevin Felter** from the Delft University of Technology for providing the different PDI samples and for involving me into this research field.
Thanks to **Prof. Dr. Schmidt-Mende** who recommended me to Bruno the same day I asked him to and for giving me the opportunity to submit my thesis.

Ein Dankeschön geht an **Felix**, der zuvor seine eigene Bachelorarbeit wohl schreiben musste, ohne dass ihm ein so guter Freund immer wieder mit Ratschlägen und Erfahrungen aushelfen und beistehen konnte.
Großer Dank gebührt **meinen Eltern**, die mich nicht erst seit Beginn meines Studiums, sondern mein ganzes Leben lang schon finanziell, bürokratisch, logistisch und nicht zuletzt auch handwerklich immer unterstützt haben.
Meinem Onkel **Christoph** möchte ich dafür danken, dass er in mir das Interesse an der Physik und Mathematik geweckt hat, ohne welches ich heute nicht dort stünde, wo ich jetzt bin.
Meiner Freundin **Leah** danke ich dafür, dass sie ein halbes Jahr und noch länger auf mich wartet und mir den größten Grund liefert, wieder zurückzukommen.